Calibration of the Massachusetts and Cape Cod Bays Hydrodynamic Model: 2000-2001

Massachusetts Water Resources Authority

Environmental Quality Department
ENQUAD Report 2004-08

Citation: Jiang, M, and M Zhou. 2004. **Calibration of the Massachusetts and Cape Cod Bays Hydrodynamic Model: 2000-2001**. Boston: Massachusetts Water Resources Authority. Report ENQUAD 2004-08. 71 p.

Massachusetts Water Resources Authority
Boston, Massachusetts

Calibration of the Massachusetts and Cape Cod Bays Hydrodynamic Model: 2000-2001

Prepared by:
Mingshun Jiang & Meng Zhou
Department of Environmental, Earth and Ocean Sciences
University of Massachusetts Boston
100 Morrissey Blvd
Boston, MA 02125

December, 2004

TABLE OF CONTENTS

LIST OF FIGURES

LIST OF TABLES

1. INTRODUCTION

1.1 Project overview

The Boston Harbor, Massachusetts Bay and Cape Cod Bay system (MBS) is important to the regional economy by serving a busy commercial harbor, a productive fishing ground, a habitat of endangered North Atlantic Right whales and a prosperous tourism industry. A healthy marine environment is also important to the more than three million people living in the surrounding area. Significant efforts have been made to clean up the Boston Harbor in the last decades. The construction of the Deer Island wastewater treatment plant and the relocation of the effluent outfall from Deer Island to 15 km offshore are among the biggest human efforts in the nation to restore an urbanized harbor.

To evaluate these restoration effort and potential impacts of the outfall relocation on the MBS, the Massachusetts Bay Program, the US Geological Survey and Massachusetts Water Resources Authority (MWRA) have funded a number of projects to study the physical-biological-chemical processes and monitor the marine environment changes in the MBS (Geyer et al., 1992; Werme and Hunt, 2002). Under these projects, numerical models have been developed to simulate and predict the physical and biological environment (Geyer et al., 1992; HydroQual, 2000; HydroQual, 2003; HydroQual and Signell, 2001; Jiang and Zhou, 2003, 2004b).

A long-term Cooperative Research Agreement was made in 2001 between the University of Massachusetts Boston (UMB) and MWRA that the UMB will maintain, enhance and apply the existing Massachusetts Bay Hydrodynamic and Water Quality Models (MB Model), and provide model run results to the MWRA for its obligations under its National Pollutant Discharge Elimination System (NDPES) permit. The hydrodynamic model in the MBS was constructed by the U.S. Geological Survey (USGS) in Woods Hole based on the ECOM-si developed by HydroQual Inc. (HydroQual) (Signell et al., 1996). The Water Quality Model was developed by HydroQual (HydroQual, 2000). HydroQual had maintained and conducted model runs up to 1999. Under the agreement between the MWRA and HydroQual, the MB Model was transferred to the UMB in 2001. To ensure successful model transfer and consistency between model results produced by different computers and model code setups, a comparison task between UMB and HydroQual model runs has been completed at the UMB (Zhou, 2002; Jiang and Zhou, 2003).

1.2 Physical setting

The MBS is a semi-enclosed embayment surrounded by the Boston metropolitan region in the north and west, and Cape Cod in the south while it is open to the Gulf of Maine (GOM) in the east (Figure 1.1). The MBS is about 100km long and 50 km wide, and has average depth of 35 m. Stellwagen Basin is the only deep basin in the MBS with a depth up to 90 m. It is bounded in the east by Stellwagen Bank with the shallowest depth of about 20 m, and is connected to the GOM through the North Passage off Cape Ann and the South Passage off Race Point.

Previous studies have indicated that the circulation in the MBS varies in response to short- and long-term local and remote forcing (Geyer et al., 1992; Signell et al., 1996). The local and remote forces include: 1) wind stresses and heat fluxes at the sea surface, 2) tides and mean surface slopes at the open boundary, and 3) freshwater runoff including outfall effluents. The yearly-mean current in the MBS is characterized by a counterclockwise circulation, which is primarily driven by both the intruding current through the North Passage associated with mean sea surface slopes, and baroclinic pressure gradients associated with the horizontal salinity and temperature gradients produced by freshwater runoff and differential heating. Tides are dominated by the semi-diurnal M_2 constituent. Tidal currents vary from 10 cm s^{-1} in Stellwagen Basin, to 50 cm s^{-1} off the tip of Cape Cod. The water column stratification varies seasonally. Stratification occurs in the spring due to both freshwater runoff and surface heating, is intensified during the summer, and reaches a maximum in the late summer. The water column is destratified during late fall due to surface cooling and increasing wind mixing, and is well mixed in the winter.

The seasonal surface slope off Cape Ann represents the southward flow of the Western Maine Coastal Current (WMCC). As early as 1927, Bigelow suggested that this current breaks into two branches at Cape Ann: one intrudes deeply into Massachusetts Bay, and another follows the outer edge of Stellwagen Bank (Bigelow, 1927; Lynch et al., 1996). During spring, the freshwater plume of the Merrimack River interacts with the WMCC, which enhances the intrusion of WMCC into the MBS (Butman, 1976). The intruding current circulates counterclockwise along western Massachusetts Bay and may penetrate into Cape Cod Bay, especially in winter and spring seasons (Geyer et al., 1992).

Our modeling study indicates pronounced seasonal variation in the circulation pattern (Jiang

and Zhou, 2004a). In western Massachusetts Bay, the currents are strongly driven by surface winds. In winter and spring seasons, northerly winds drive a southward coastal current thus creating a counterclockwise circulation that is consistent with the annual mean pattern (Geyer et al., 1992). In summer and early fall, predominant southwest winds produce offshore Ekman transport and coastal upwelling, which induce an overall northward coastal current along the upwelling front near the western coast. This is confirmed by the moored Acoustic Doppler Current Profiler (ADCP) current measurements at the US Geological Survey buoys (Butman et al., 2002) and the modeling study (Jiang and Zhou, 2004a). The coastal upwelling and downwelling have also been discussed in previous studies (e.g., Geyer et al., 1992; HydroQual and Signell, 2001).

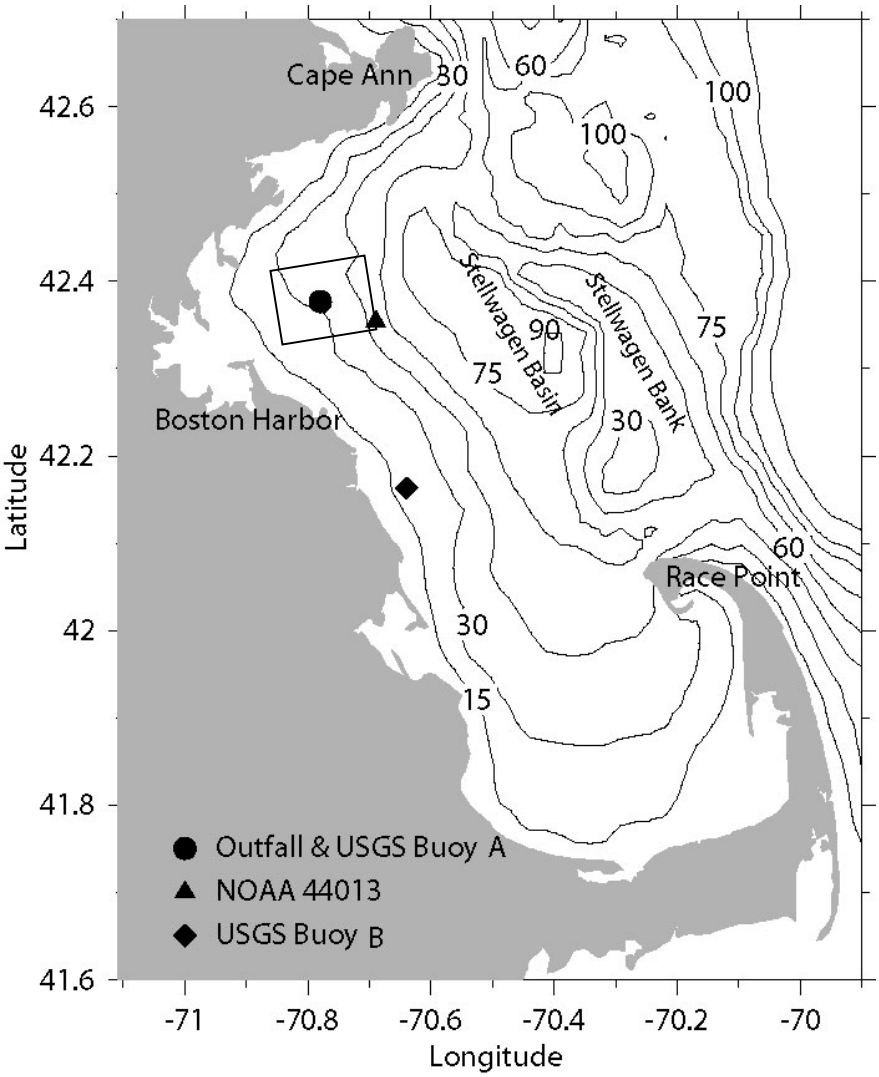

Figure 1.1 Bathymetry in the Boston Harbor, Massachusetts Bay and Cape Cod Bay system (MBS). The black box indicates the Massachusetts Water Resources Authority (MWRA) nearfield monitoring area.

2. MODEL DESCRIPTION

A brief model description is presented in this section. More details can be found in Signell et al. (1996) and HydroQual and Signell (2001). The model implementation is the same as the simulations for 1998-99 by HydroQual and Signell (2001), except the improvements in the open boundary treatment described in section 2.4.3.

2.1 Numerical schemes

The Massachusetts Bay and Cape Cod Bay hydrodynamic model is based on the semi-implicit Estuarine, Coastal and Ocean Model (ECOM-si), which is a derivative of the Princeton Ocean Model (POM) (Blumberg and Mellor, 1987; Signell et al., 1996). The model solves the three-dimensional primitive equations using a terrain-following coordinate (sigma coordinate) and a semi-implicit scheme developed by Casulli et al.(1990) in the calculation of the free sea surface elevation to avoid the splitting of barotropic and baroclinic modes. The integration of passive tracer equations is further enhanced with a flux-corrected anti-diffusion algorithm (Smolarkiewicz et al., 1984).

The vertical turbulent closure is the Mellor-Yamada 2 ½ scheme (Mellor and Yamada, 1982) with modifications by Galperin et al.(1988), while the horizontal mixing is parameterized as formulated by Smagorinsky (1963). In addition to turbulent mixing, a background vertical mixing is chosen to be 5×10^{-6} m^2 s^{-1}. Moreover, a Shapiro filter is applied to velocity field every 2 hours to remove the 2 grid-length variability (Shapiro, 1975).

2.2 Model domain and grids

The model domain extends into the GOM including the Merrimack River, the largest source of fresh water in the region (Figure 2.1). This configuration minimizes the disadvantage of insufficient data in the construction of open boundary conditions. The bottom topography is smoothed with the maximum depth of 140 m near the eastern boundary and the minimum depth of 3 m near coastal areas to avoid treating flooding and drying grids.

The model has 68×68 grids with the grid spacing approximately from 600 m in Boston Harbor to about 6 km along the open boundary. Vertically, the model has 12 sigma levels with

upper three levels located at 0.01, 0.04 and 0.1 sigma depths, and the remaining 9 layers at a 0.1 sigma depth interval evenly distributed over the rest of the water column.

2.3 Time step

A time step of 207 seconds is used throughout the entire simulation between years 2000 and 2001. Though the semi-implicit scheme used for the sea surface elevation avoids the instability of an explicit scheme produced by the gravity waves, the model time step is limited by the advective Courant-Levis-Frederick (CFL) condition, which requires the modeled time step less than or equal to grid spacing divided by current speed ($\Delta t \leq \Delta x/U$). A time step of 207 seconds is a very conservative choice. The model was executed stably.

2.4 Forcing

2.4.1 Surface forcing

The surface forcing includes wind stresses, incoming short wave radiation, net outgoing long wave radiation, sensible heat fluxes and latent heat fluxes. The freshwater input at the surface is set to zero because no measurements of precipitation and evaporation were available from offshore stations. The precipitation was measured at Logan Airport but not evaporation, which is more difficult to measure directly. Moreover, even if it had been measured at Logan Airport, the data would not be appropriate for the bay because it was measured about 60 m above land surface. Wind stresses and heat fluxes are calculated based on meteorological measurements made at NOAA buoy 44013 and solar radiation measurements at Woods Hole Oceanographic Institution (Figure 2.2-2.3). Because there is no humidity measurement at these stations, relative humidity measurements from Logan Airport are used in the calculation of sensible and latent heat fluxes. Wind measurements at the NOAA buoy are missing during a period from January 22 to April 26, 2001. This data gap is filled with wind measurements at Logan Airport. The wind stresses are then calculated using the Large and Pond (1981) formulation, and long wave radiation, sensible and latent heat fluxes are calculated using the formulation developed by Weller et al.(1995).

The meteorological forcing is typical of mid-latitude regions: in fall and winter, northerly wind is dominant with a wind speed higher than 10 m s^{-1}; and in spring and summer, southerly

wind is more frequent with an overall wind speed less than 5 m s^{-1}. In 2000, the lowest air temperature reached -15°C during the mid-January, and highest air temperature reached approximately 25°C between July and August. In 2001, a similar weather pattern was observed except that the winter was mild, and the air temperature was seldom below -5°C.

Solar radiation penetrates into the water column. The absorption of short wave radiation is computed as a function of the water depth, i.e.,

$$I(z) = I_0 \exp(-k_e z) \tag{2.1}$$

where I_0 is the solar radiation at the sea surface, k_e is the light attenuation coefficient, which is derived from historical field measurements in the bay (HydroQual and Signell, 2001), z is the water depth, and $I(z)$ is the solar radiation at depth z.

2.4.2 Freshwater inputs

There are four major land sources of freshwater: the Merrimack River, Charles River, Neponset River, and MWRA sewage effluents (Figure 2.4 and 2.5). Among them, the Merrimack River is the largest with an averaged flux of 200 m^3 s^{-1} and the other sources are much smaller with an averaged flux of ~20 m^3 s^{-1}. All river discharges have strong seasonality with the maximum runoff between late March and early May. The effluent from the MWRA Deer Island facility was discharged at the Deer Island outfall site before September 6, 2000, and has been completely diverted to the new outfall site in Massachusetts Bay thereafter. The effluent from the MWRA Deer Island facility is nearly constant throughout the year. The runoff from Mystic River is included in the model freshwater source though it is small. The sewage flux from South Essex plant flow is not included because it is less than 1.3 m^3 s^{-1}, much smaller than the MWRA effluent flow limit. The river runoff data are not available after September, 2001; they are substituted by data between October and December, 2000.

2.4.3 Open boundary conditions

The open boundary conditions required by the model include surface elevations, temperature and salinity. Surface elevations consist of tidal and low frequency components. The low frequency surface slope is associated with the geostrophic coastal currents perpendicular to the open boundary. The tidal elevation is derived from the tidal model of Lynch and Naimie (1993).

An objective interpolation procedure is used to derive the temperature and salinity along the open boundary, which is similar to the interpolation procedure in the previous simulations (HydroQual and Signell, 2001). The interpolation software, called OAX, is developed by Bedford Institute of Oceanography (http://www.mar.dfo-mpo.gc.ca/science/ocean/coastal_hydrodynamics/oax.html). The interpolation is made by weighting available data onto the open boundary based on a specified statistical correlation function of horizontal distance, depth and time, so that the statistical interpolation error is known. Data from the National Marine Fisheries Service (NMFS), MWRA, EcoHAB project and National Ocean Data Center (NODC) were compiled based on latitude, longitude, depth, and time. For example, the monthly station maps in April and in August for 2000-2001 are shown in Figures 2.6-2.7. The monthly data coverage in space and time varies significantly, and are summarized in Table 2.1.

A new calculation procedure of the low frequency surface elevation along the open boundary is developed in the 2000-2001 simulation. In the 1992 simulation, the low frequency surface elevation was computed based on available current measurements at a series of mooring stations (Signell et al., 1996). In later simulations, when mooring current data were not available, the 1992 low frequency surface elevation data were used with fine-tuning (HydroQual and Signell, 2001). In the new procedure for the 2000 simulation, we first interpolate the temperature and salinity along the open boundary, and then the low frequency surface elevation gradient is inferred from the density field based on the geostrophic balance relation with a reference depth of 100 m or the ocean floor if it is shallower than 100m. The absolute sea surface elevation requires a known absolute sea surface elevation at one point on the open boundary. We simply assume that the elevation at the outer coast of Cape Cod is zero throughout the year. This assumption needs to be improved when gauge data are available in the future. In the 2001 simulation, because there are very few temperature and salinity data available for the open boundary interpolation, we use the two-year (1998-1999) averaged sea surface elevation data.

The transects of interpolated temperature, salinity, density and the relative interpolated error estimate (RMS) along the open boundary in April and in August, 2000 are shown in Figures 2.8a and 2.8b, respectively. The RMS estimates in April on the open boundary are lower than that of August because the station coverage in April is better than that of August (Figures 2.6 and 2.7). In April, the water column is partially mixed except in areas near the northern coast where freshwater runoff creates strong horizontal and vertical salinity gradients. In August, both

surface heating and freshwater runoff produce a warm and fresh surface layer. The reverse vertical density gradients in the interpolated results during April, 2000 and 2001 are unrealistic, which is likely caused by the sampling station array biases (Figures 2.8 and 2.9). Overall, the interpolated temperature and salinity distributions on the open boundary well represent the seasonal cycles of the water column stratification in the GOM throughout the year.

The estimated surface elevations for year 2000 are shown in Figure 2.10. The horizontal gradients determine the long-term geostrophic currents into or out of the model domain. Note that the flat elevation in January is caused by no observations during that month. In the rest of the year, the results indicate an overall inflow in the northern portion of the open boundary and a permanent outflow in the southern portion of the open boundary. The strongest intruding current occurs in the spring and early summer, which is produced by the peak freshwater runoff in the spring and strong horizontal temperature gradients in the summer. The interpolated seasonal patterns of temperature, salinity and currents are consistent with the modeling results for the GOM region (Xue et al., 2000).

Table 2.1 Quality of data coverage for objective interpolation in 2000 and 2001

Year	**Month**	**Rating***
2000	January	-
	February	-
	March	-
	April	+
	May	-
	June	0
	July	-
	August	-
	September	-
	October	0
	November	0
	December	-
2001	January	-
	February	-
	March	-
	April	+
	May	-
	June	-
	July	-
	August	0
	September	+
	October	+
	November	0
	December	-

* Definitions of symbols: + (good), 0 (fair) and - (poor).

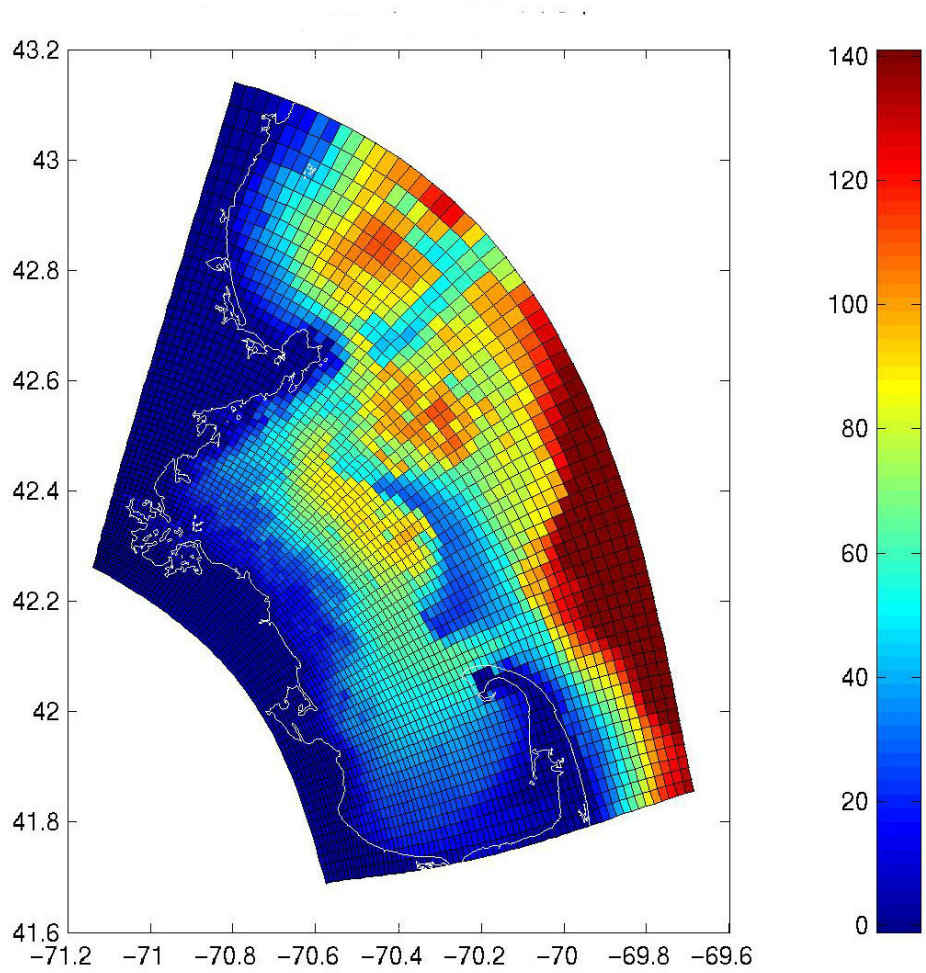

Figure 2.1 Model domain and grids in the MBS.

(a)

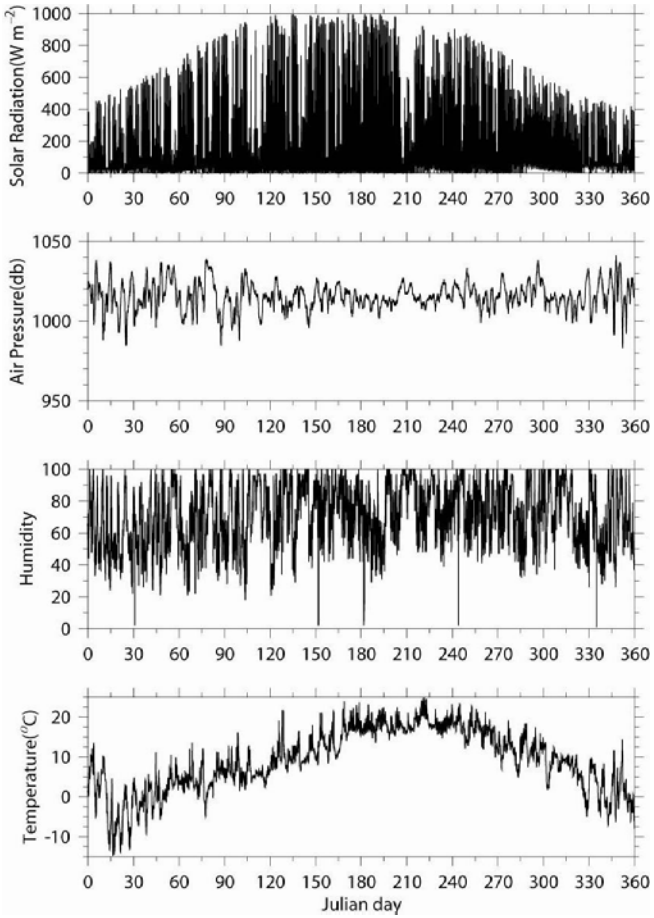

(b)

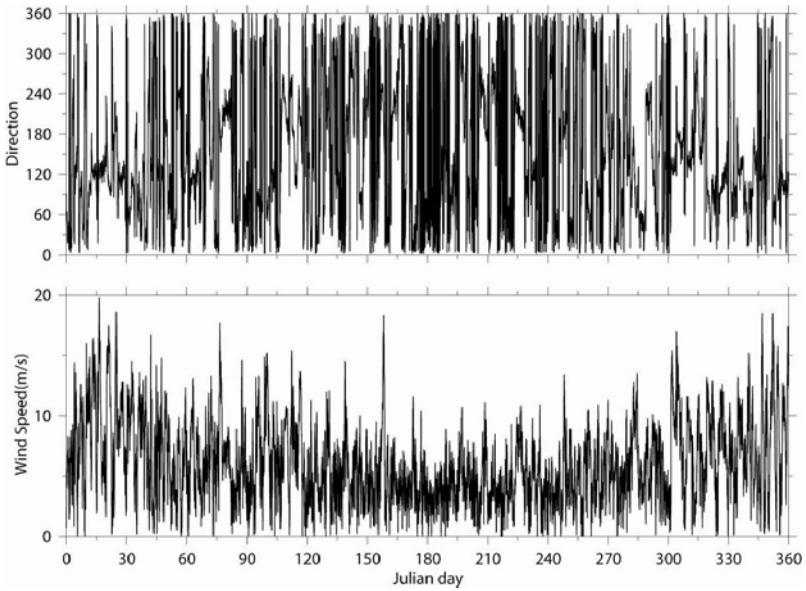

Figure 2.2. Meteorological forcing at NOAA station 44013 in 2000: (a) solar radiation, air pressure, humidity, and air temperature, and (b) wind speed and direction.

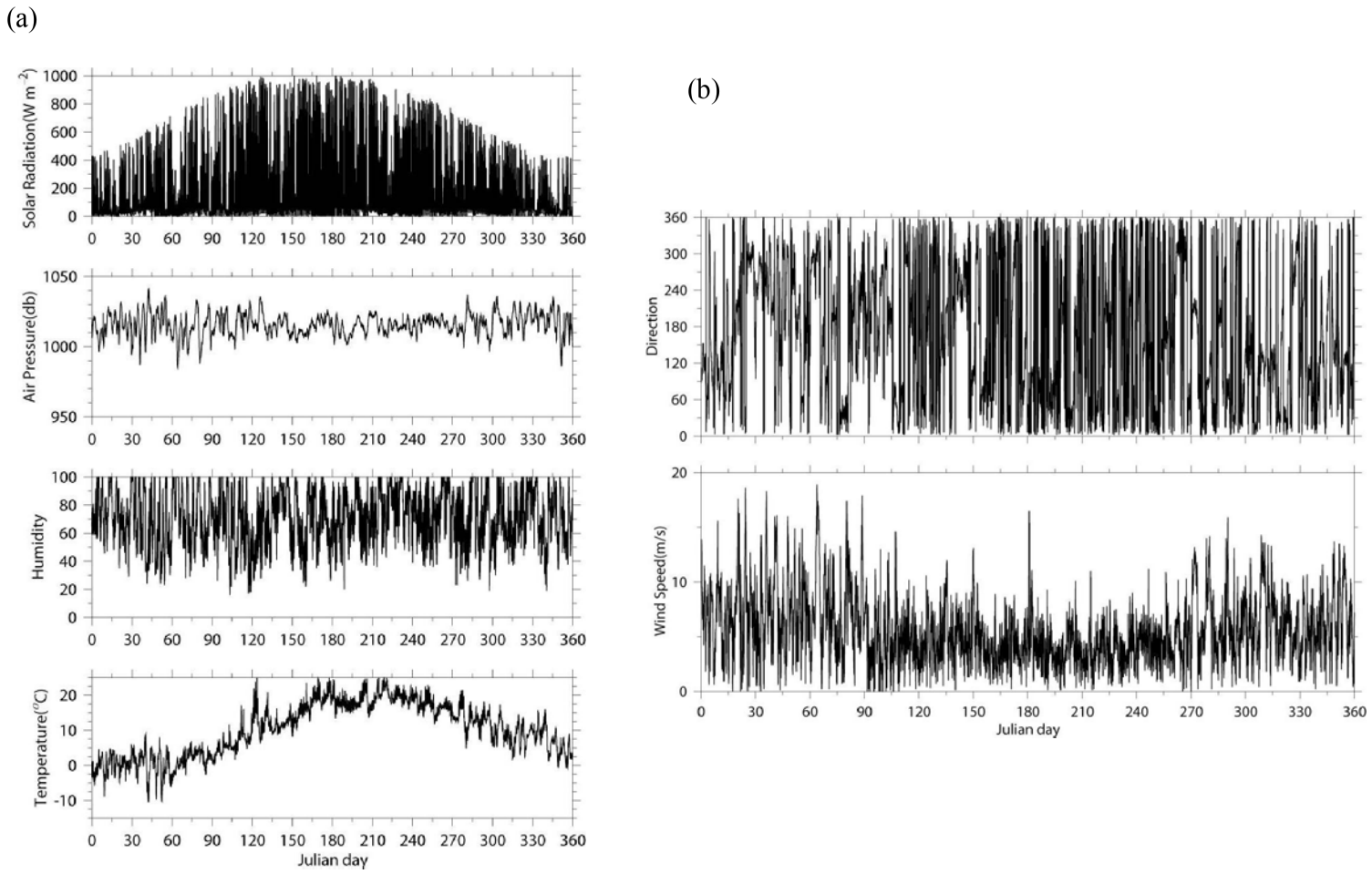

Figure 2.3. Meteorological forcing at NOAA station 44013 in 2001: (a) solar radiation, air pressure, humidity, and air temperature, and (b) wind speed and direction.

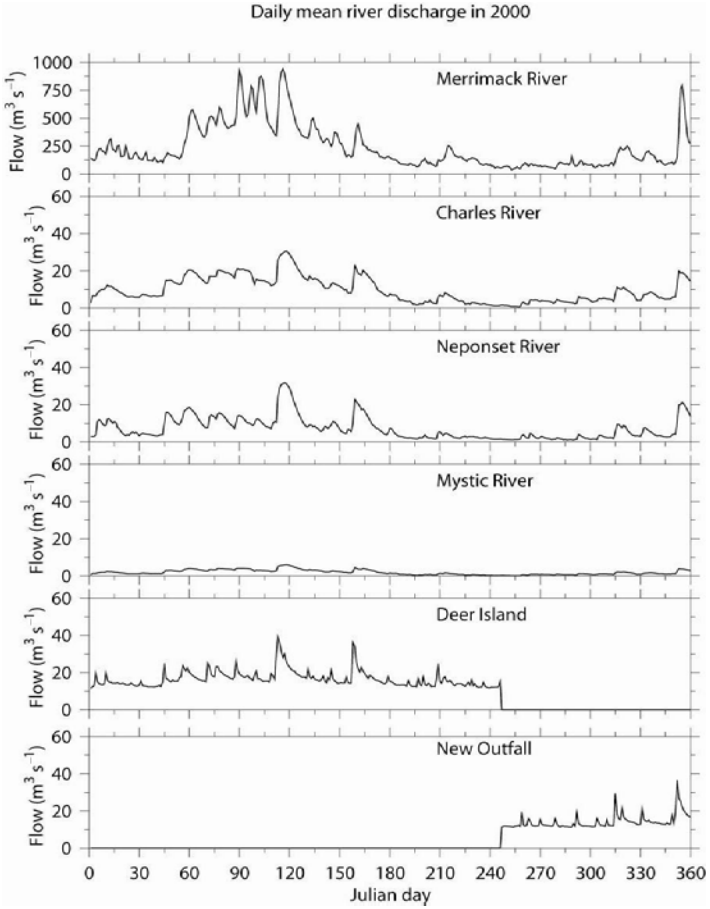

Figure 2.4 Daily river discharges in 2000.

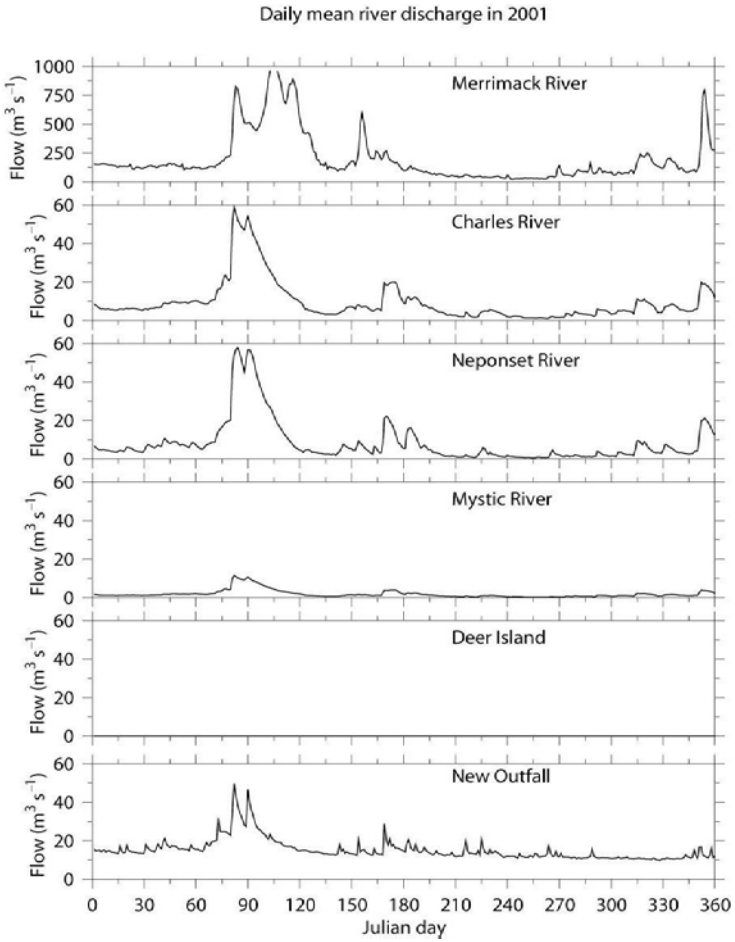

Figure 2.5 Daily river discharges in 2001.

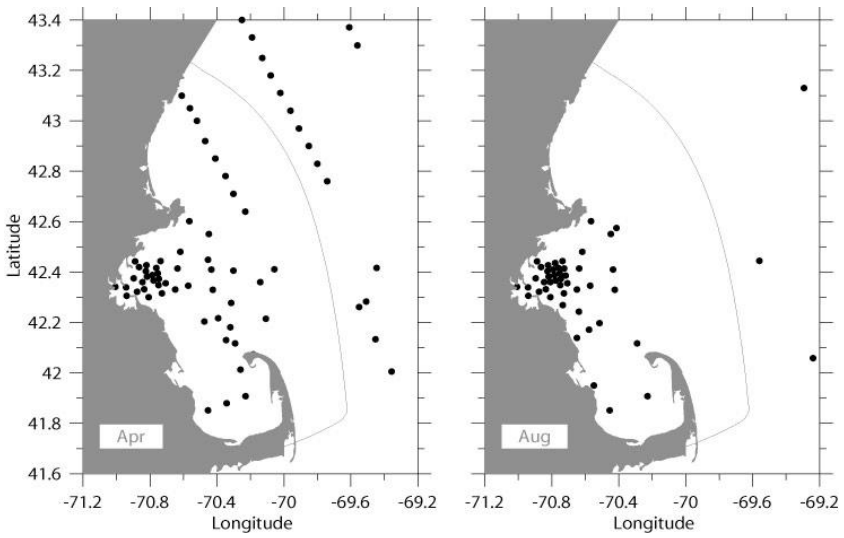

Figure 2.6 Station maps of available data in April and August, 2000.

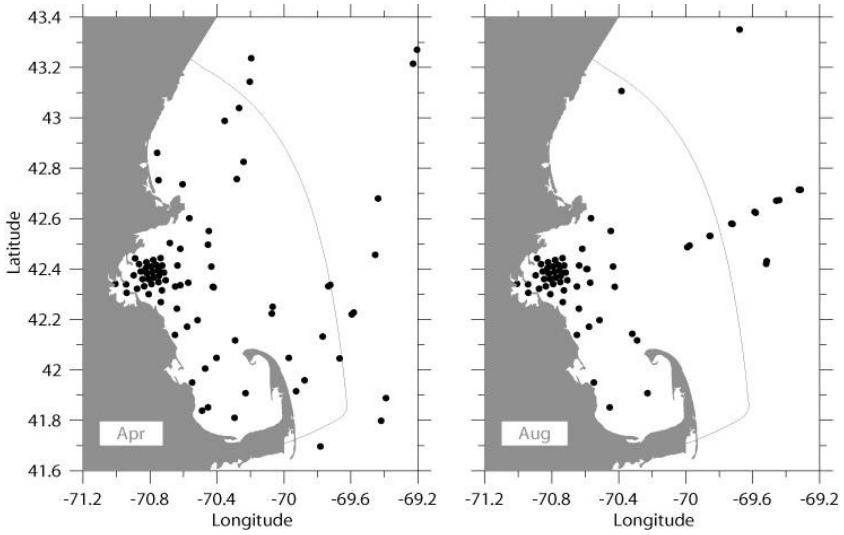

Figure 2.7 Station maps of available data in April and August, 2001.

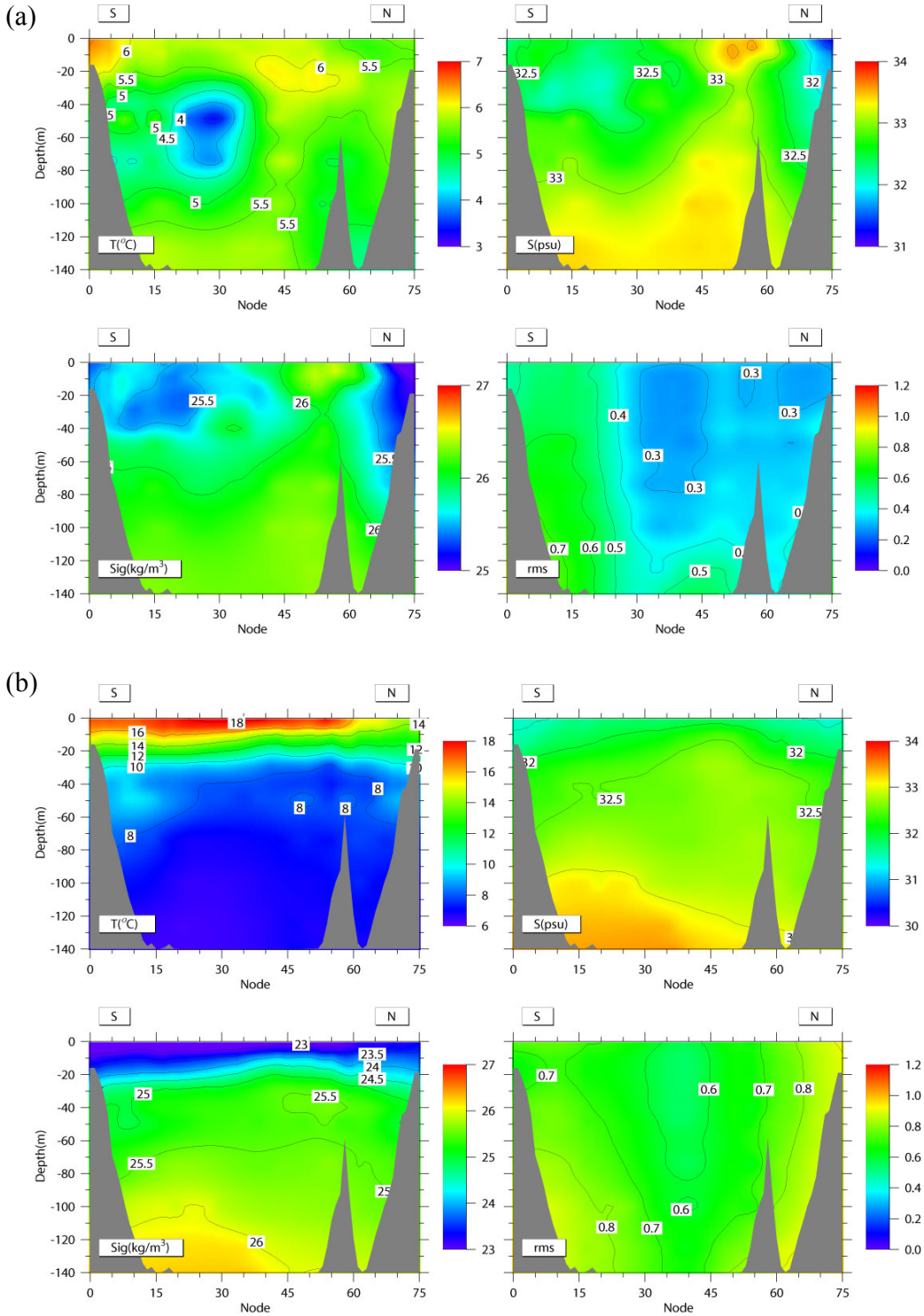

Figure 2.8 Open boundary conditions of temperature, salinity, σ_t and rms errors in (a) April and (b) August, 2000.

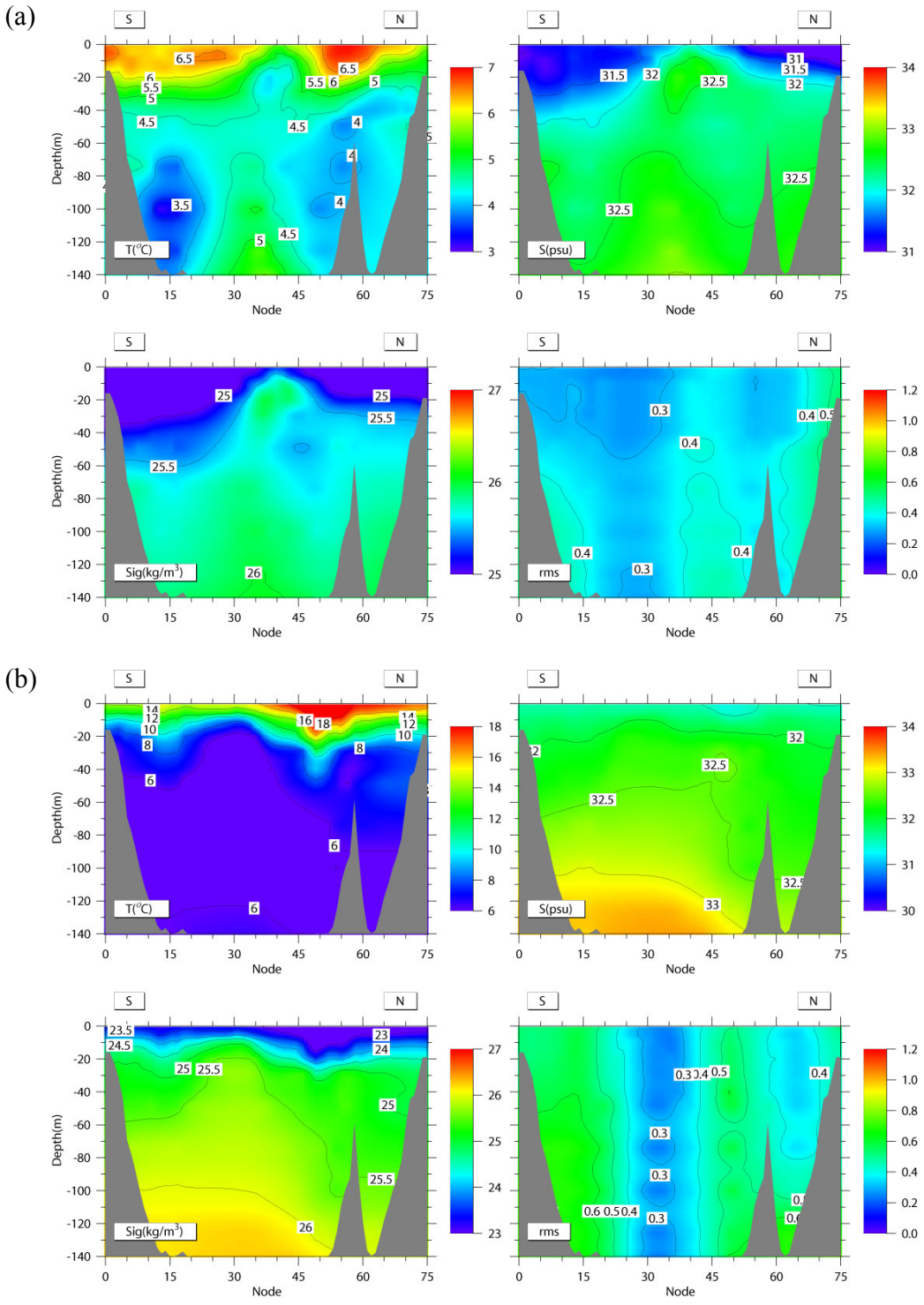

Figure 2.9 Open boundary conditions of temperature, salinity, σ_t and rms errors in (a) April and (b) August 2001.

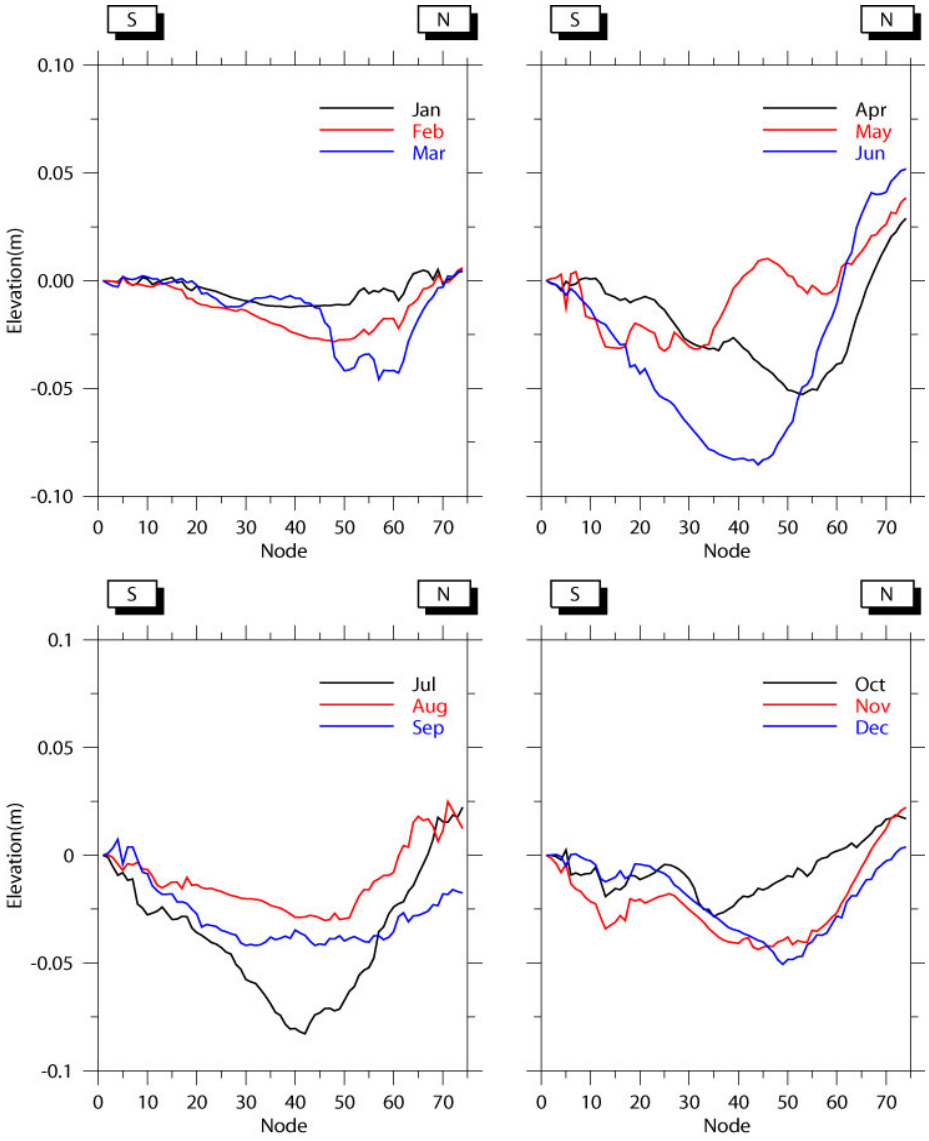

Figure 2.10 Monthly sea surface elevations at the open boundary in 2000.

3. CALIBRATION

3.1 Time series

3.1.1 Cruise data

The twelve stations chosen for this comparison represent the sampling network (Figure 3.1). These stations are organized into four groups: a) group 1 consisting of Stations F26, F27 and F29 along the eastern boundary of Massachusetts Bay, b) group 2 consisting of Stations F31, N01 and N10 near the MWRA outfall site in the northwestern Massachusetts Bay, c) group 3 consisting of stations F07, F01 and F02 in southern Massachusetts and Cape Cod Bays, and d) group 4 consisting of Stations N04, N07 and F17 in the offshore region near the MWRA outfall site, northern Massachusetts Bay. Among these stations, F07, N04 and N07 are on the shelf slope and F17 is in Stellwagen Basin.

The comparisons between observations and model results of temperature and salinity in 2000 are shown in Figure 3.2 where the depths of surface and bottom observations at each station correspond to the third and 12th sigma levels in the hydrodynamic model, respectively. The model results compared well with observations at these stations. In particular, the model captures the strengths and timings of stratification in summer and de-stratification in fall. In the spring and summer, the two major discrepancies between model and observations are: 1) the model underestimates the salinity at both the surface and bottom during late June and early July, and at the surface during August in the nearfield; and 2) the model underestimates both the surface and bottom water temperature at station F01 and F02 and the surface water temperature at station N01 and N10 during the summer. Such discrepancies can be caused by intensive upwelling and downwelling processes in responses to the wind variability during the summer, which produce strong fluctuations in both observed and modeled temperature, salinity and positions of fronts at these shallow stations. The difference between modeled and observed salinity is unlikely due to the zero air-sea fresh water exchange (precipitation and evaporation), because the modeled bottom salinity is also lower than the observed which should not be affected by the surface fluxes. During the winter, the temperature is overestimated at N10 and F02 compared to the observations in early February, and underestimated at F26 and F27 in February. Overall, the modeled temperature field tends to have less horizontal gradients than the

observed field in February, 2000.

The modeled temperature and salinity fields in 2001 well agree with the observed temperature and salinity fields (Figure 3.3) except for possible outliers in the observed records. For example, the temperature at F27 and F29 was recorded at 17~18°C in mid June, about 3-5 ºC higher than the modeled temperature,. Also the salinity at F26 was recorded at 28‰ in early April, about 2 ‰ lower than the modeled salinity. It is also lower than the CTD downcast measurement 29.1‰ at 2m. This low salinity may be due to the freshet from rivers inputs in the GOM (Libby et al., 2002). Because of the high variability in wind, current, temperature and salinity fields that can lead to mismatch between modeled and observed temperature and salinity, the observed data well support the modeled ones.

3.1.2 Buoy data

The comparisons between the modeled and measured temperature and salinity at buoy stations in 2000 are shown in Figure 3.4. The modeled results follow the seasonal cycles of observations very well. The modeled temperature well resembles the observed temperature at both mooring sites A and B, particularly in winter, though the model misses a strong cooling event in late June and early July, which lasted about 2 weeks. Though this cooling event was observed from water column temperature, it was not observed in the air temperature data (Figure 2.2), suggesting that this cooling event is most likely produced by the cold water intrusion from the GOM. Missing this cooling event in the modeled results is likely caused by a lack of spatial and temporal coverage of observations along the open boundary. The modeled surface salinity values at sites A and B are approximately 0.7‰ and 0.5‰, respectively, lower than the observed since June. At site A, the model underestimates the strength of the major upwelling/downwelling events during the summer as indicated from the observed surface temperature while the model captures most upwelling/downwelling events at site B. The modeled vertical temperature and salinity gradients at site B are stronger than observed during downwelling events, which can be interpreted by either underestimates of vertical mixing in the model during strong downwelling, or the unresolved spatial variability of wind fields, bathymetry and coastal geometry. For example, temperature and salinity measurements exhibit much stronger variability at Buoy B in the shallow water than those of Buoy A in the deep water during the summer.

The overall good agreement between modeled and observed currents at Buoy A and B holds

in winter, spring and fall 2000 (Figure 3.6 and 3.7). Similar to previous year model runs, the model experiments encountered difficulties in reproducing the currents and stratification during summer, especially at Buoy B (Signell et al., 1996; HydroQual and Signell, 2001). Signell et al (1996) indicated that intensive upwelling/downwelling and freshwater runoff produce small spatial scale circulation patterns sensitive to the location and timing of events. The coastal upwelling and downwelling are usually associated with coastal fronts with lateral scales of internal Rossby radii of 5-7 km in summer (Jiang and Zhou, 2004). The instability of these coastal fronts occurs frequently, which may lead to cross-shelf jets and rapid displacements of fronts (Barth, 1989). Such wind-induced baroclinic instability and jets are hard to predict because of their chaotic nature.

The subtidal signals from remote regions are another aspect of uncertainties that are not accounted for in the model. The periods in the boundary forcing include tidal periods and the time durations between two monthly surveys. The forcing with timescales between the tidal periods and the month-interval is missing in our boundary conditions due to a lack of observations. These signals are more important when wind and the horizontal gradients of water properties become stronger during summer.

Comparisons of temperature and salinity at buoy stations between modeled and observed results in 2001 show similar agreement to those of 2000. The modeled temperature and salinity well follow the seasonal trends in the observations at both stations throughout the entire year (Figure 3.5). It is also obvious that the time series of modeled temperature have missed the fluctuations with periods of 10-20 days observed at site A. The modeled surface salinity at Buoy A is overall lower than the observed in April, May, and late June and agrees with observed in summer and fall periods. Surface temperature and salinity were not measured at site B.

The modeled currents in 2001 resemble the observed currents at Buoys A and B similar to those of 2000 (Figures 3.8 and 3.9). The agreement between the modeled and observed currents is best in the winter and worst in the summer. Again, these disagreements can be caused by mesoscale processes and the limited temporal and spatial coverage of monitoring stations used for constructing boundary conditions.

3.2 Spatial distributions

3.2.1 Surface patterns in 2000

Surface pattern comparisons are made for the spring cruise in early April 2000 and the summer cruise in August 2000 (Figure 3.10) in which the survey had the best spatial coverage in Massachusetts Bay. A typical cruise usually takes 5-7 days to cover the nearfield and farfield stations. Considering that the advective distance is approximately 40 km at a current speed of 10 cm s^{-1} for 5 days, a 5-day cruise does not provide a synoptic map of any observed variable, or a mean value over the observation period. To reduce these spatial and temporal biases, we choose modeled variables centered on the median date of each survey period and average these modeled variables over a M_2 tidal period for the comparison.

The observed temperature field between March 31 and April 3, 2000 is quite homogeneous in Massachusetts Bay except Boston Harbor. Relatively cold water is found in southern Massachusetts Bay and Cape Cod Bay. Similar to the temperature field, the salinity field is very uniform in Massachusetts Bay. The lowest salinity is found in Boston Harbor and near Cape Ann.

The modeled temperature field on April 2 2000 basically resembles the observed temperature field with more complicated mesoscale patterns. For example, in the modeled temperature field, the relatively warm water exists in Plymouth Harbor and along the eastern side of Cape Cod Bay. A stripe of cold water is found across the middle of Cape Cod Bay (Figure 3.10a), which may represent the cold water found in the observations (Figure 3.2). The modeled salinity field also shows more mesoscale features, especially the east-west gradients, than the observed. The salinity values of waters in Boston Harbor and off Cape Ann are approximately 1‰ below the observed.

The prevailing wind was northerly or northwesterly during the period between August 16 and 20, 2000, which produced the downwelling along the western coast (Figure 3.10c and d). A coastal front was formed with warm water accumulating within 10 km of the western coast. These features are well represented in both modeled and observed temperature fields. Though the fresh water in Boston Harbor is present in both the modeled and observed salinity fields, modeled results show the detailed fresh water plume extending from the mouth of Boston Harbor southward along the coast, which demonstrates the strength and advantage of the modeling work. The modeled temperature also shows a warm filament extending from Plymouth Harbor toward the South Passage, while the observed temperature does not show this feature because there was

no station there. In general, the modeled and observed patterns of both temperature and salinity fields agree very well.

3.2.2 Cross-sections in 2000

The temperature and salinity along two cross-sections are compared in Figures 3.12 and 3.13. The summer downwelling situation along section 1 (Scituate to Stellwagen Basin) is represented by the data collected in August 16-20, 2000 (see Figure 3.10 for the horizontal distribution). The spring, summer and fall distributions along section 2 (Hull to Cape Ann) are represented by data collected from three cruises conducted from March 31 to April 3, from August 16 to 20 and from October 3 to 5.

During March 31-April 3 2000, the water was already stratified primarily from freshwater runoff. Relatively fresh and warm water lies within the top 5-10 m near western coast (Figure 3.13a and 3.13b). Both model and observations show a similar vertical structure though the subsurface salinity from the model is approximately 0.5 ‰ higher than the observed. The spatial discrepancies between modeled and observed temperature and salinity also include: near the entrance of Boston Harbor, the modeled salinity is lower than the observed; and in the North Passage, the modeled salinity is higher than the observed. These discrepancies may result from contouring the observations between sparse sampling stations. For example, the distance between station F26 and its nearest station (F22) is approximately 15 km, 2-3 times larger than the internal Rossby Deformation Radius of 5-7 km, which represents horizontal scales of meso-scale features. The observations did not resolve the mesoscale features while the model does. Overall, the modeled and observed temperature patterns agree reasonably well.

The downwelling events observed in August 16-20 (Figures 3.10c and d, 3.12a and b, 3.13c and d) are well reproduced by the model. While the water is strongly stratified in most areas, a deep warm water body is accumulated in the nearshore area on both sections 1 and 2. Since section 1 (Scituate to Stellwagen Basin) consists of only 4 sampling stations, the coastal front is not well defined in the observation. The modeled salinity is generally approximately 0.5‰ lower than the observed in western Massachusetts Bay, and the modeled temperature is approximately 1°C lower than the observed in the mixed layer. Similar conclusions can also be applied to the October 3-5 comparison.

3.2.3 Surface patterns and cross-sections in 2001

In the 2001 comparison, the modeled temperature and salinity on August 27, 2001 are compared with the observed between August 26 and 31, 2001. During the survey period, the southerly wind overwhelmingly dominated, setting up an upwelling favorable condition along the west coast. Modeled and observed temperature and salinity show the upwelling extending from Cape Cod to Salem (Figures 3.11a and b). The warm water is pushed offshore to the deep areas. The upwelling near western coast can also be clearly identified in the temperature distribution along section 2 (Hull to Cape Ann) (Figure 3.14a). Though modeled surface temperature is approximately 1°C higher than the observed along Section 2 (Figure 3.11), the agreement between modeled and observed temperature and salinity fields is quite good. Along Section 1 the modeled salinity also agrees with data, though in Stellwagen Basin the modeled halocline is shallower than the observed.

3.3 Correlation analysis for currents at Buoy A and B

The statistical correlations between modeled and observed currents are also studied at two buoy stations A and B in 2000 (Figure 3.15 and 3.16). A 60 hour filter is applied to both modeled and buoy data prior to the computation of correlations for filtering out high frequency motions. Over a year average, the correlations at Buoy A are approximately 0.42 and 0.6 for the north-south (N-S) and the east-west (E-W) current components, respectively; and the correlations at Buoy B are approximately 0.57 and 0.72 for the north-south (N-S) and the east-west (E-W) components, respectively. It is obvious that the flow pattern at Buoy A is more complicated by the interaction between the intruding flow from the GOM and the outflow from Boston Harbor than the flow at Buoy B. At either Buoy A or B, the depth contours are generally in the N-S direction. The low correlation for the E-W component indicates the randomness associated with the cross-shelf currents produced by the instability of the coastal fronts and current jets. Overall, there is no phase drift between observed and modeled currents at either station.

The correlations between modeled and observed currents are also computed by seasons (Figure 3.17), in which winter is defined from December to February, spring from March to May, summer from June to August, and fall from September to November. Consistent with our previous discussions, the correlation is higher in fall and winter, and lower in summer; higher at Buoy B and lower at Buoy A; and higher in the N-S direction and lower in the E-W direction. A

phase shift of approximately 0.5 day is found in these correlations. The N-S correlation during the winter exhibits a second peak of 0.4 with a time lag approximately 3.7 days. Further study is needed to understand these time lags and the causes for the low correlations in the E-W direction.

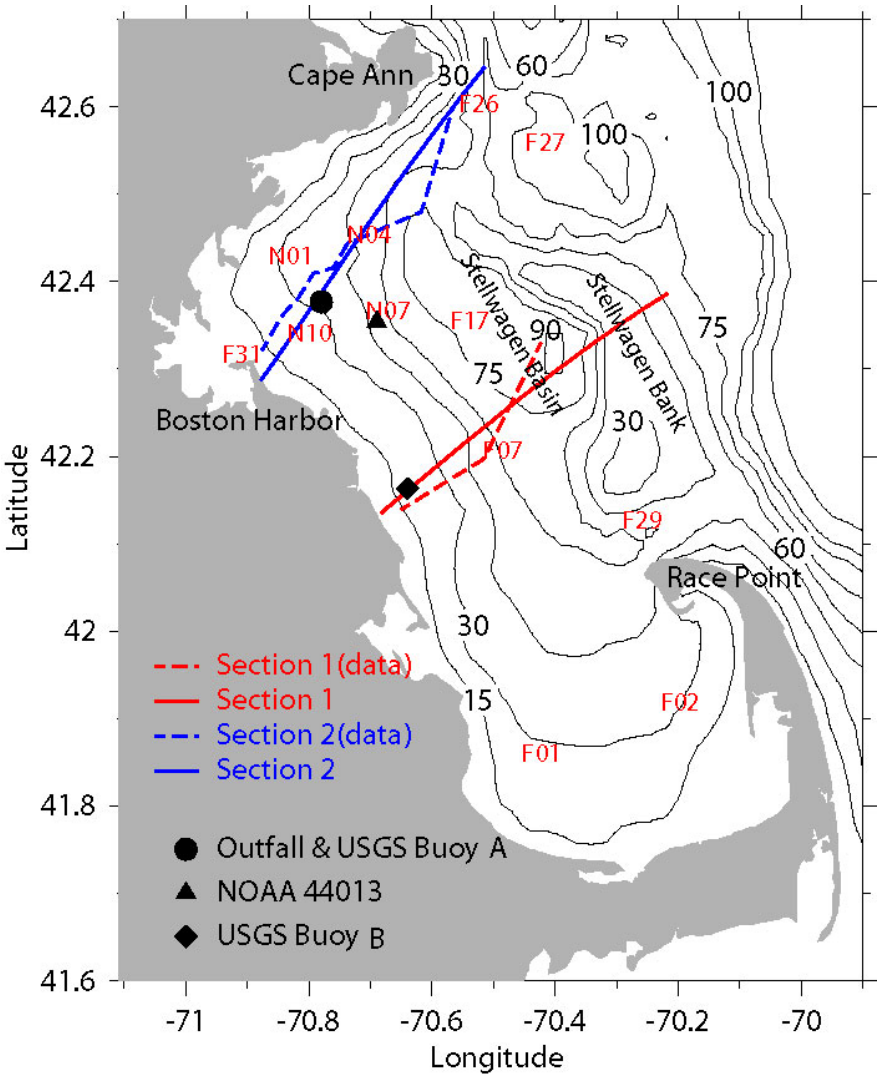

Figure 3.1 Stations and cross-sections used for model calibration.

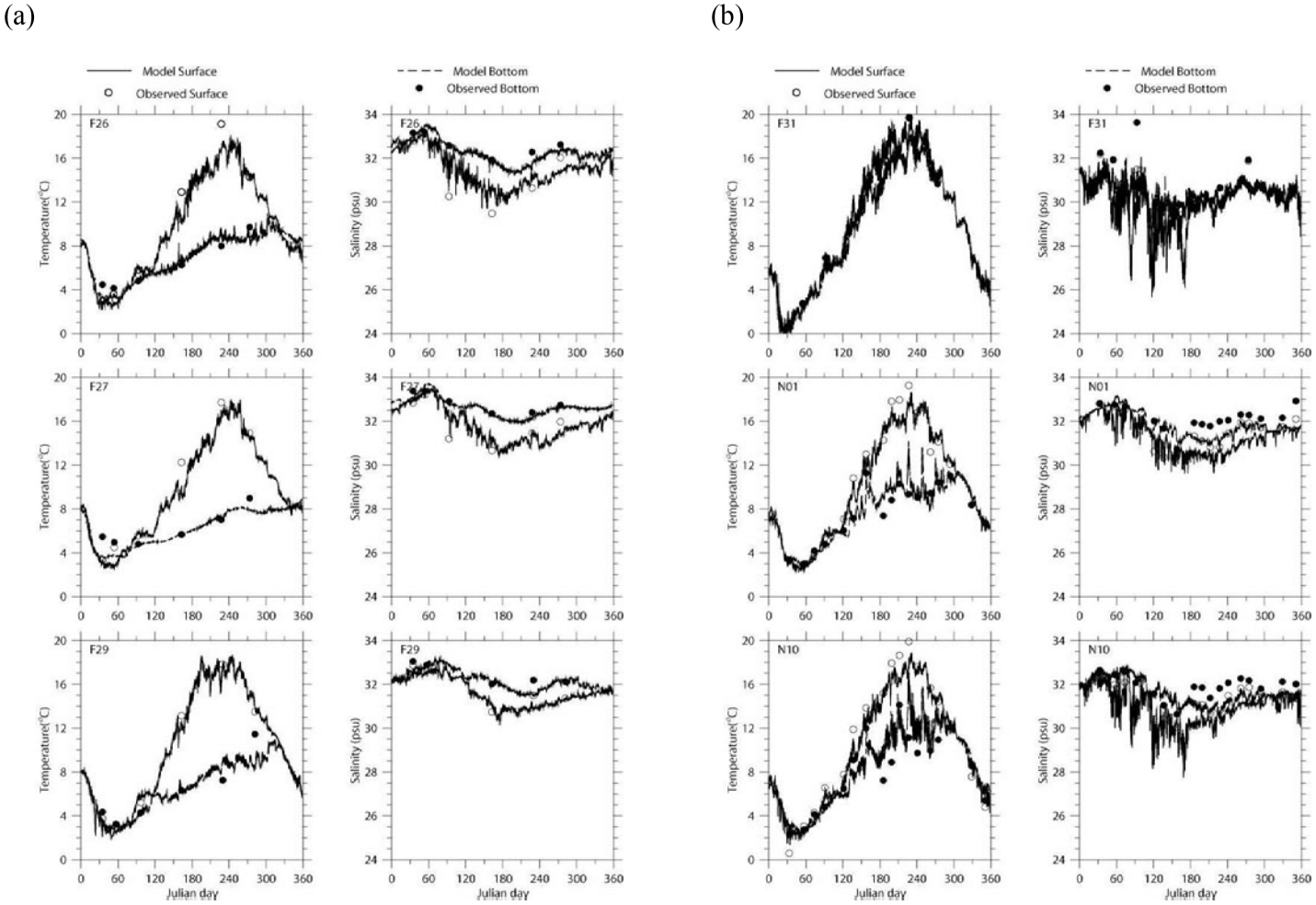

Figure 3.2. The comparisons between modeled and observed temperature and salinity at selected stations in 2000. (continued on next page)

(c)

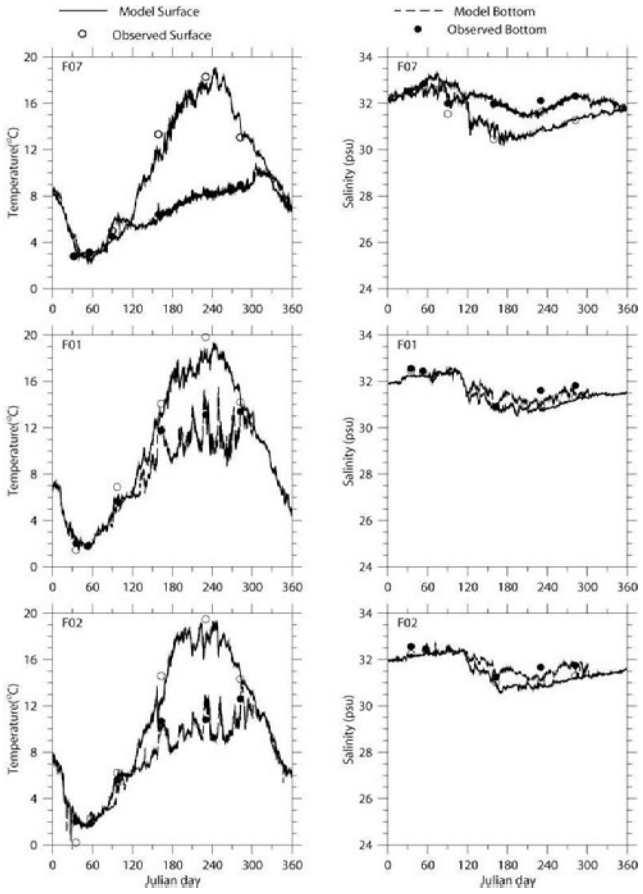

(d)

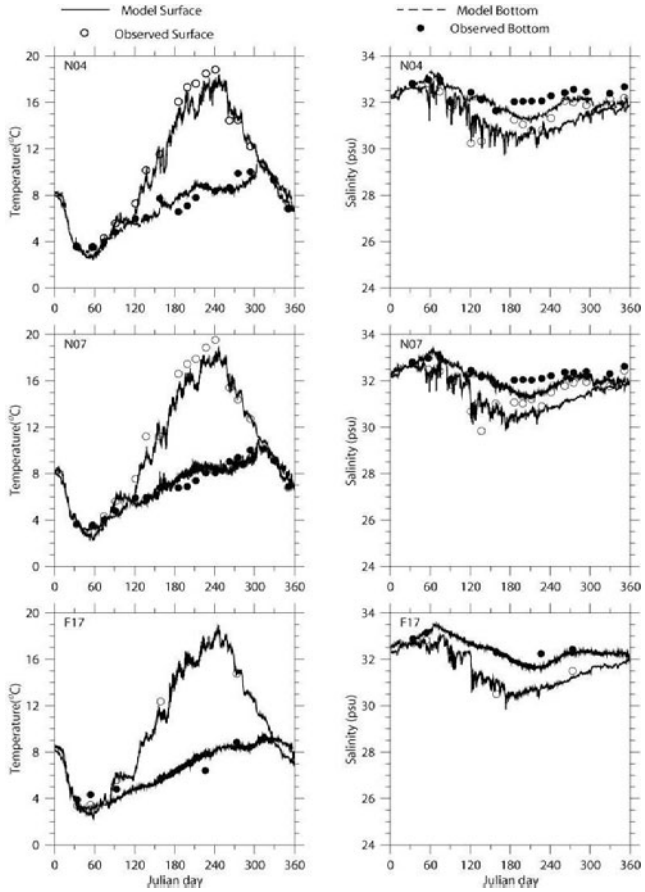

Figure 3.2. Continued.

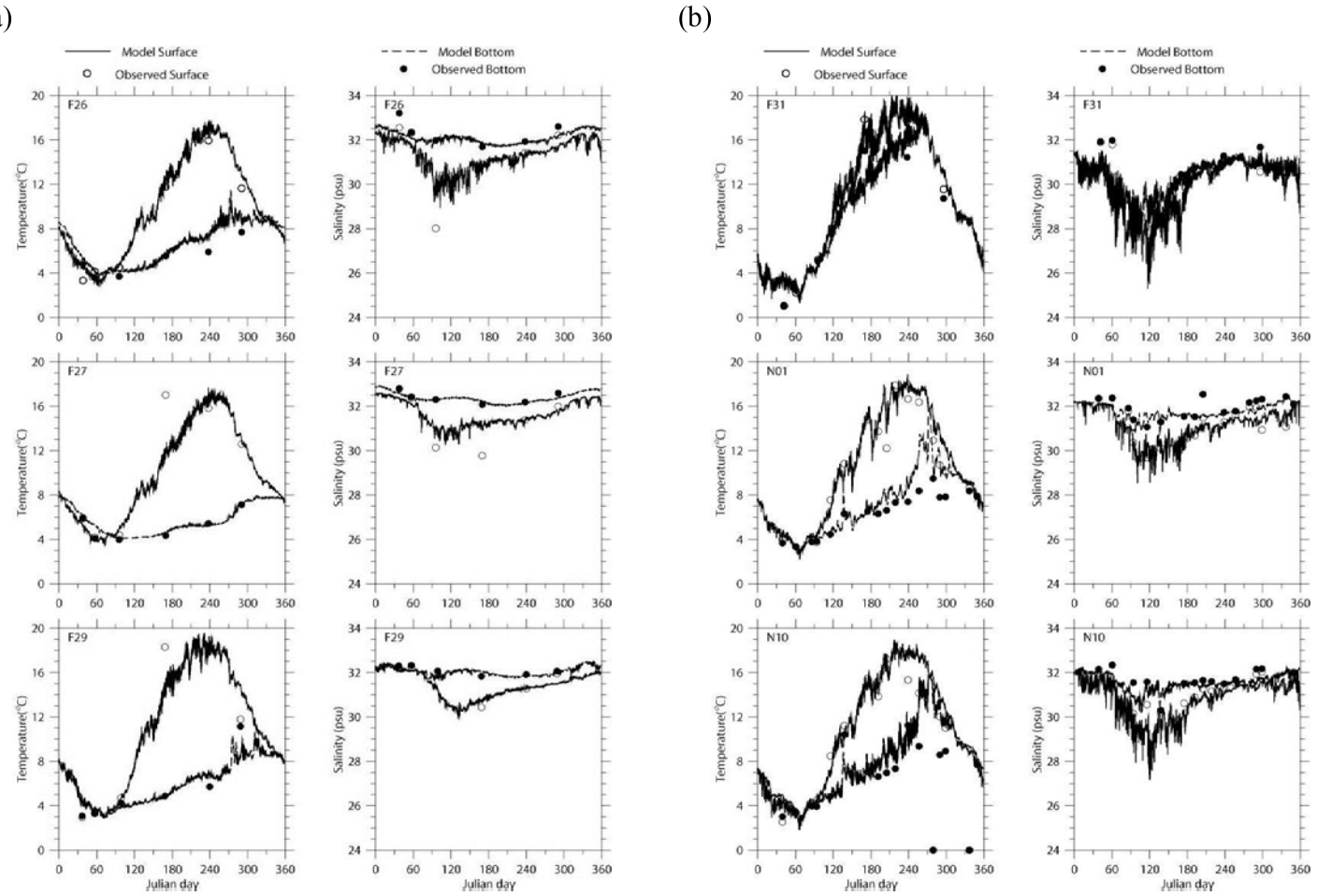

Figure 3.3. The comparisons between modeled and observed temperature and salinity comparisons at selected stations in 2001. (to be continued on next page)

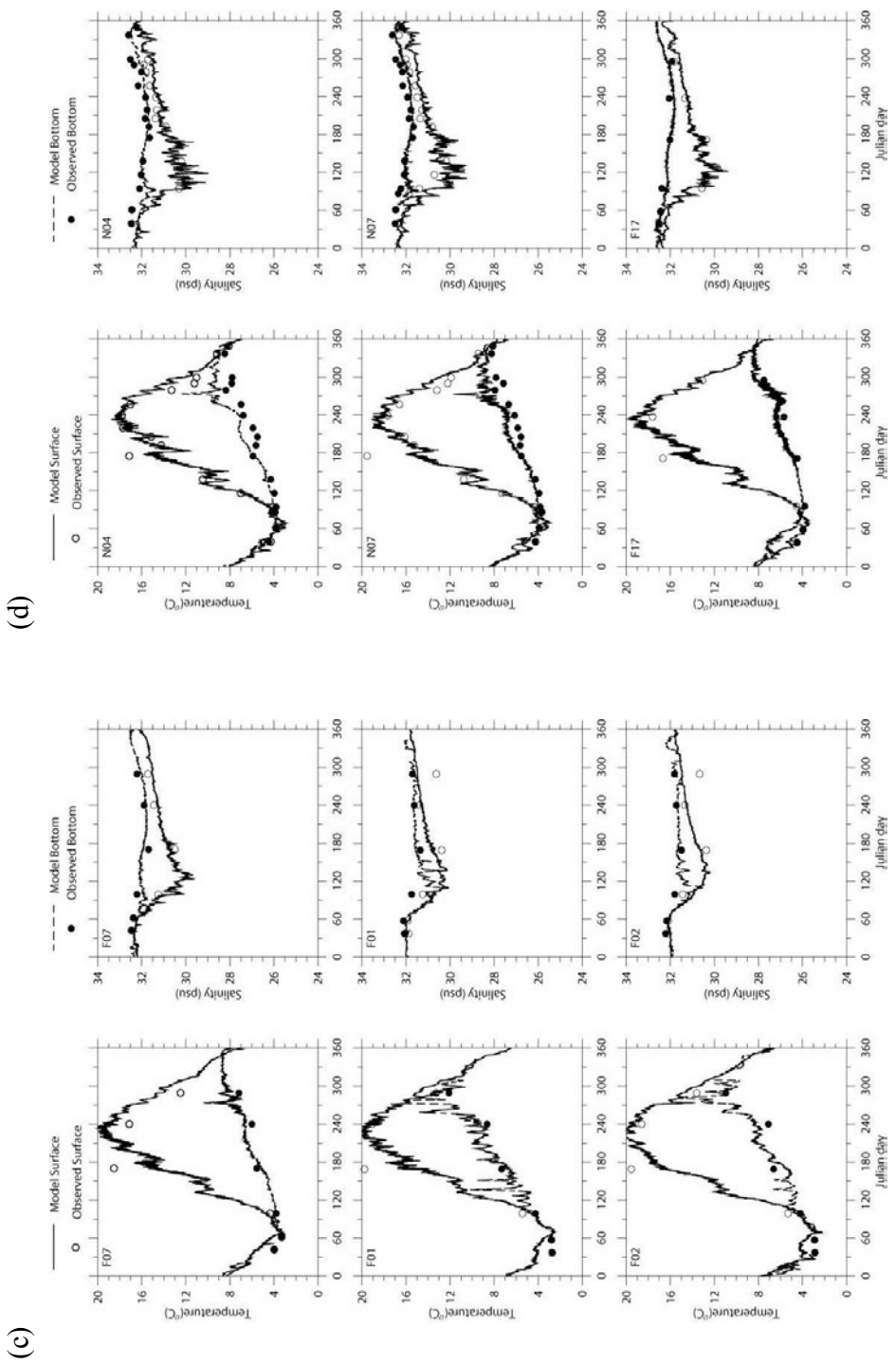

Figure 3.3. Continued.

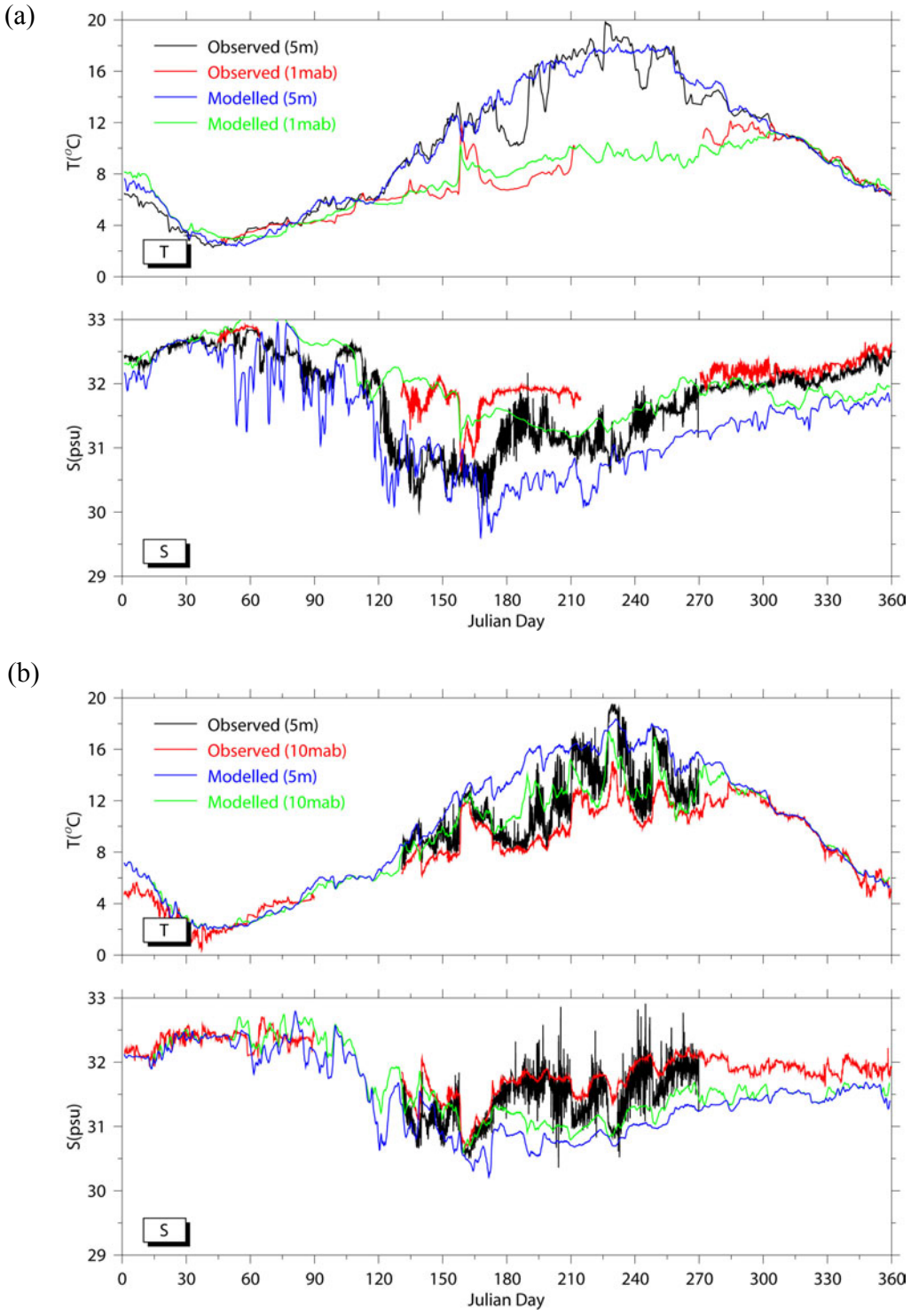

Figure 3.4. The comparisons between modeled and observed temperature and salinity at (a) USGS Buoy A and (b) USGS Buoy B in 2000. "mab" means meters above bottom.

(a)

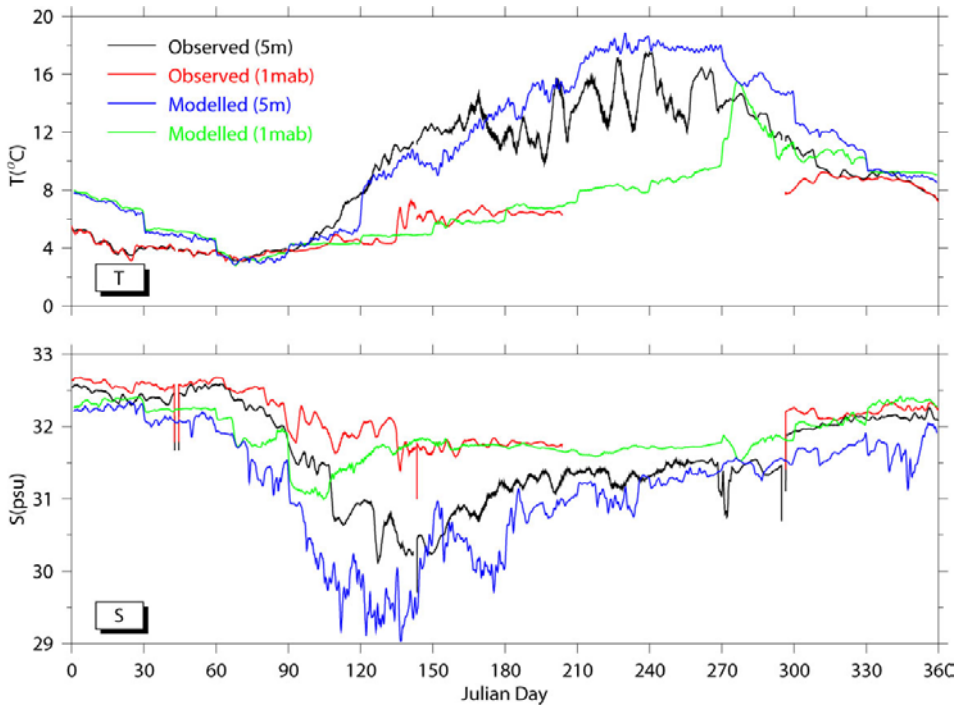

(b)

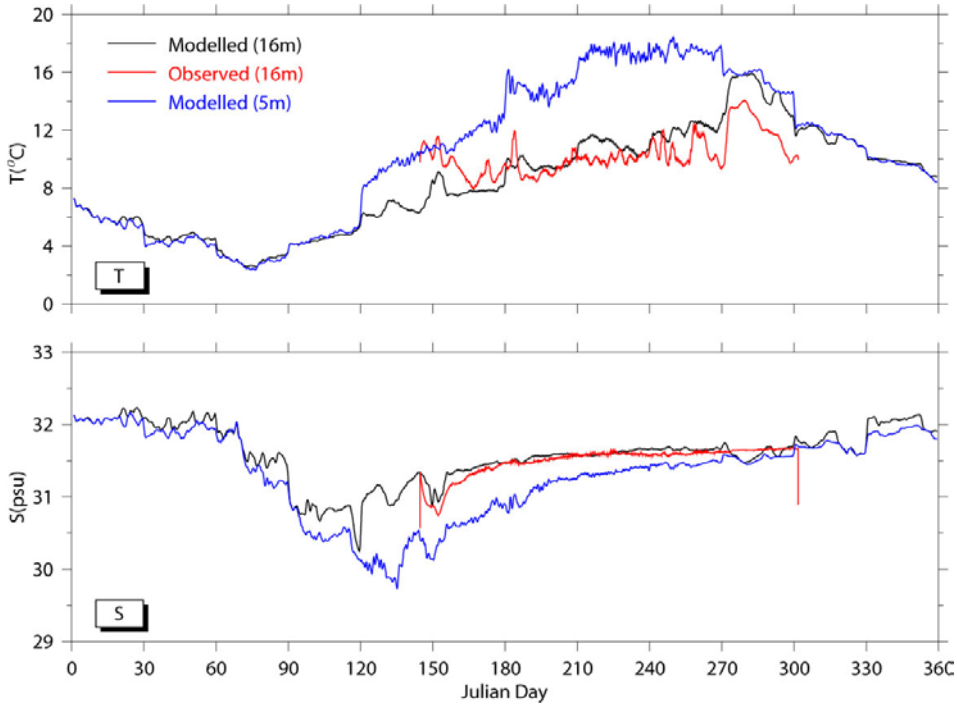

Figure 3.5. The comparisons between modeled and observed temperature and salinity at (a) USGS Buoy A and (b) USGS Buoy B in 2001. "mab" means meters above bottom.

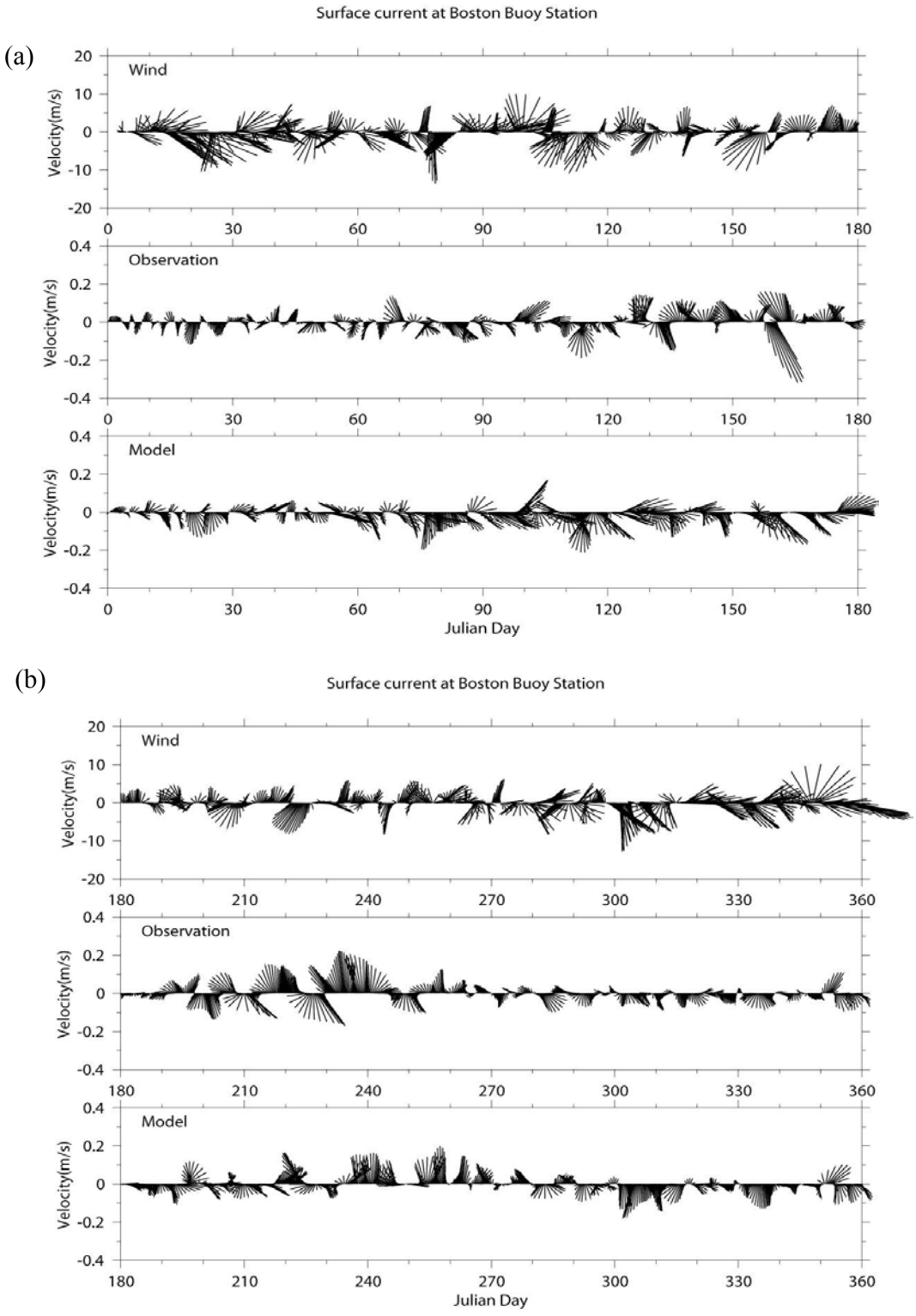

Figure 3.6. Wind at NOAA 44013 and surface currents at USGS Buoy A in (a) January-June 2000 and (b) July-December 2000. Both wind and currents are filtered with a 60 hour Lanczos filter.

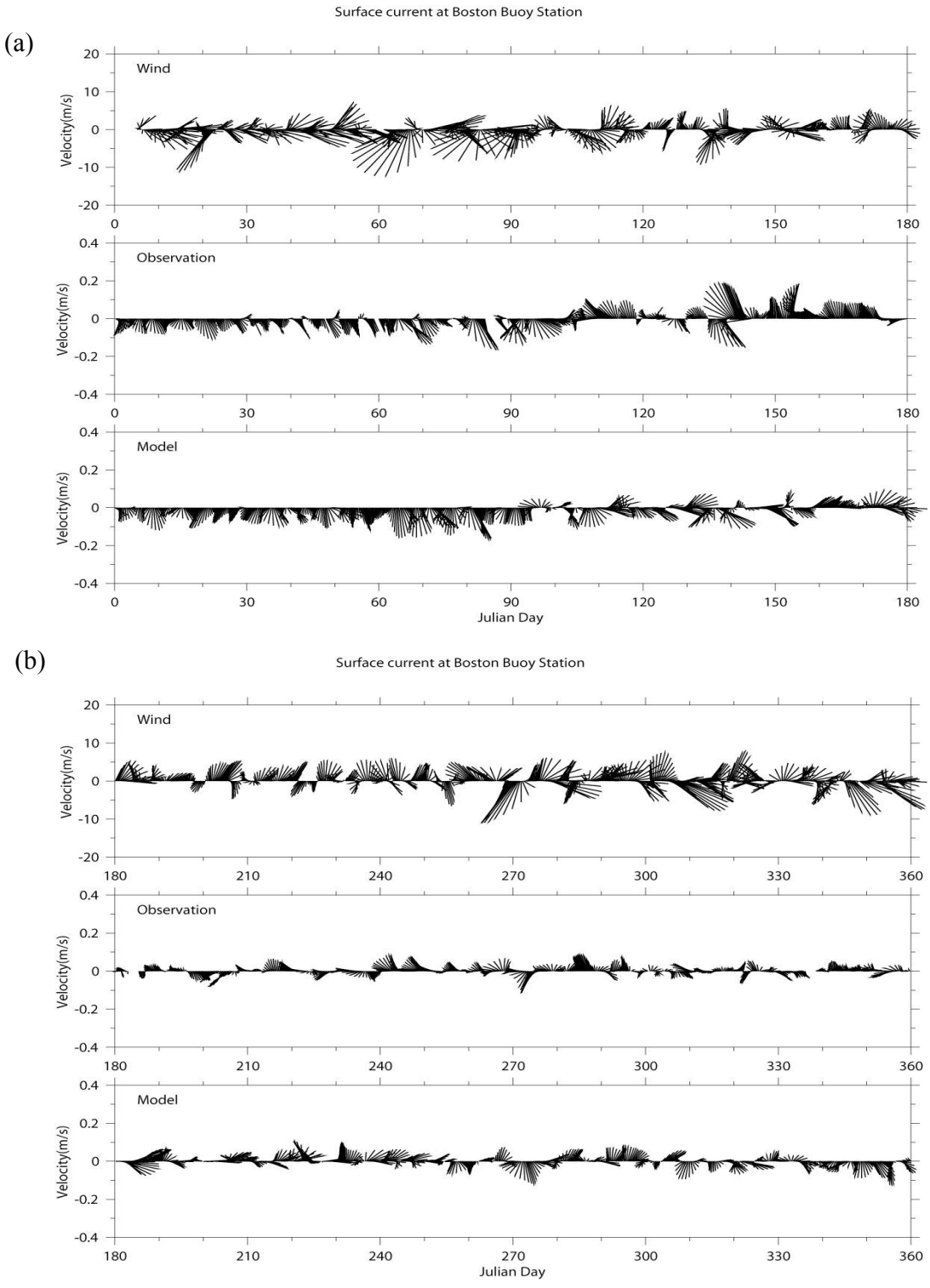

Figure 3.7. Wind at NOAA 44013 and surface currents at USGS Buoy A in (a) January-June 2001 and (b) July-December 2001. Both wind and currents are filtered with a 60 hour Lanczos filter.

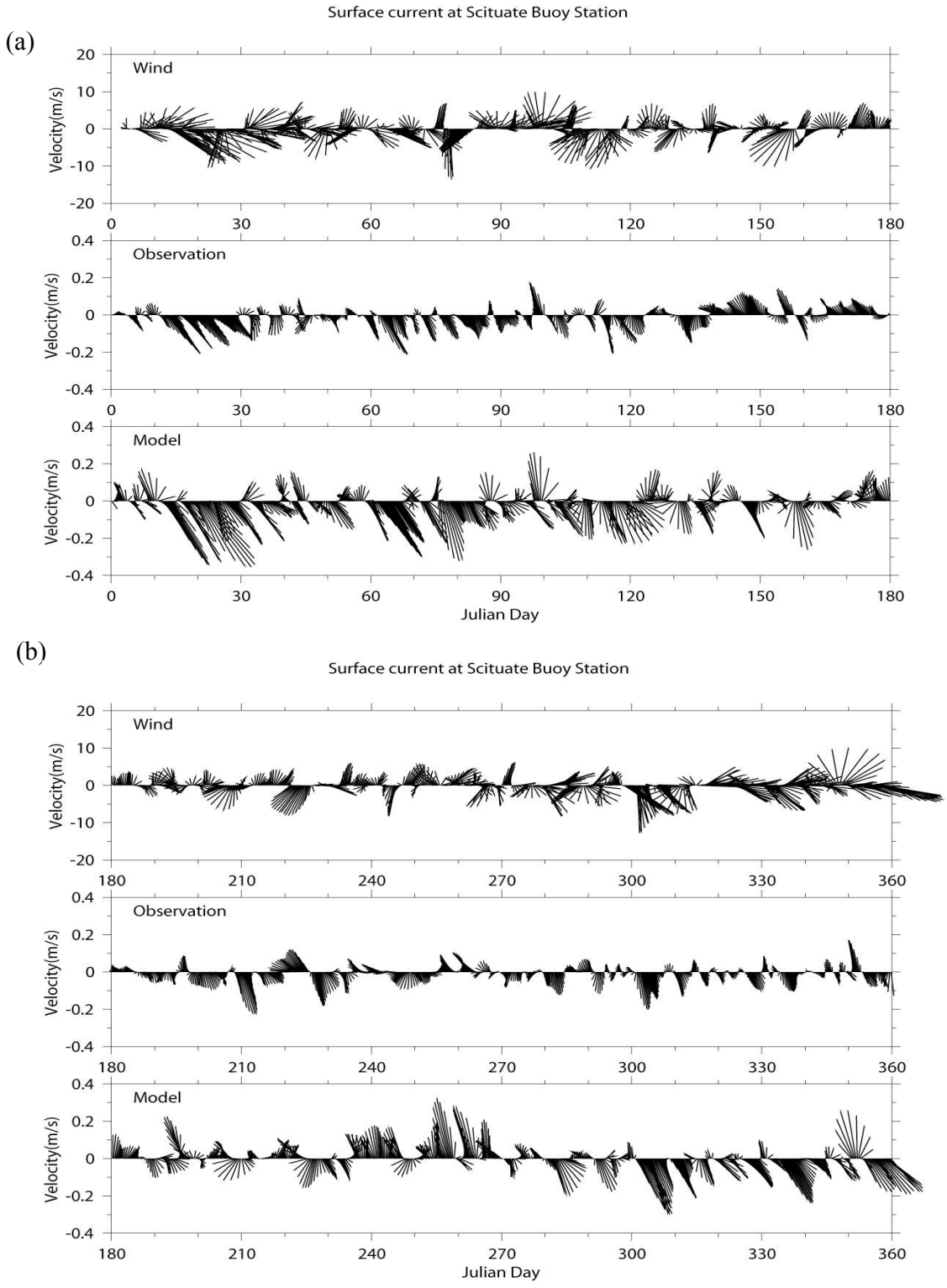

Figure 3.8. Wind at NOAA 44013 and surface currents at USGS Buoy B in (a) January-June 2000 and (b) July-December 2000. Both wind and currents are filtered with a 60 hour Lanczos filter.

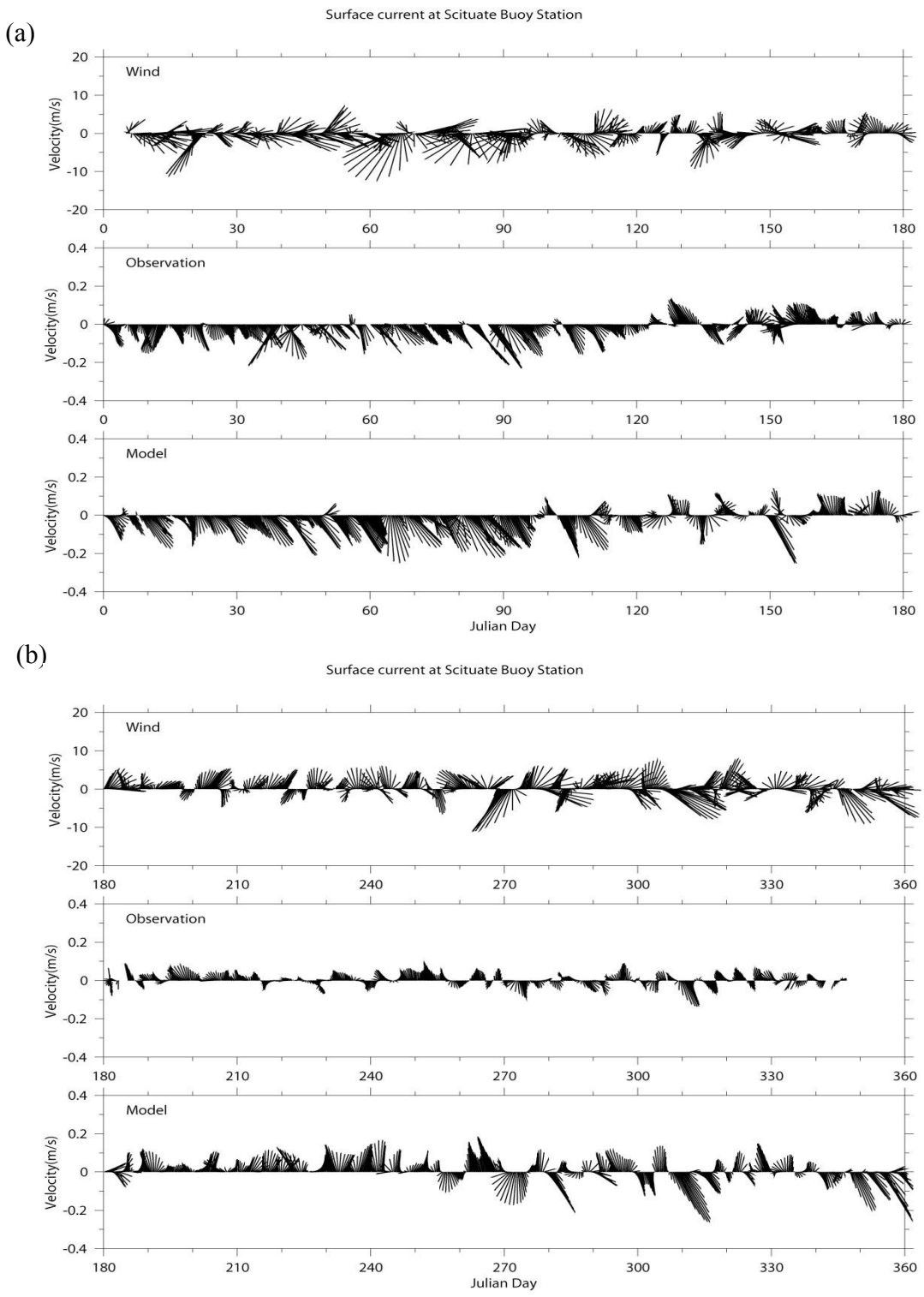

Figure 3.9. Wind at NOAA 44013 and surface currents at USGS Buoy B in (a) January-June 2001 and (b) July-December 2001. Both wind and currents are filtered with a 60 hour Lanczos filter.

(a)

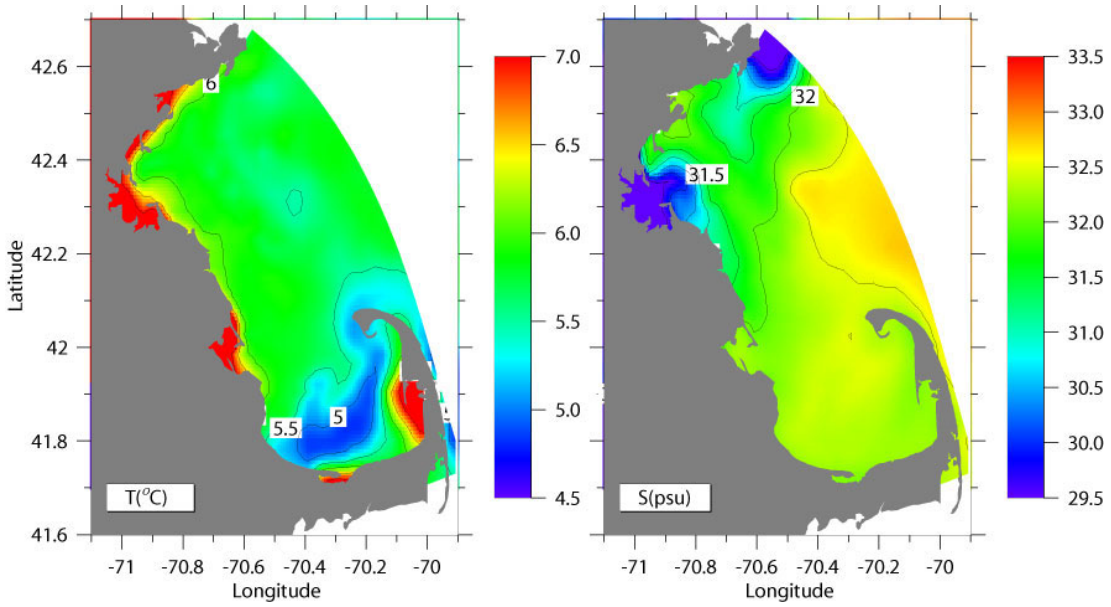

(b)

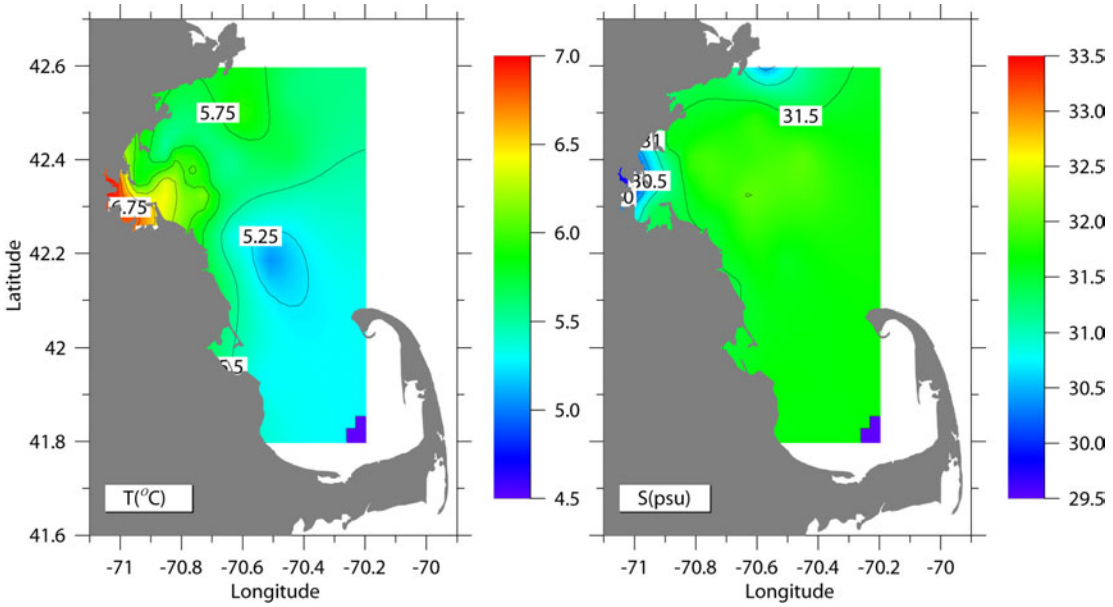

Figure 3.10. Comparisons between modeled and observed surface temperature and salinity for selected cruises in 2000: (a) modeled results on April 2, (b) observations in March 31-April 3, (c) modeled results on August 17, and (d) observations in August 16-20. (to be continued on next page)

(c)

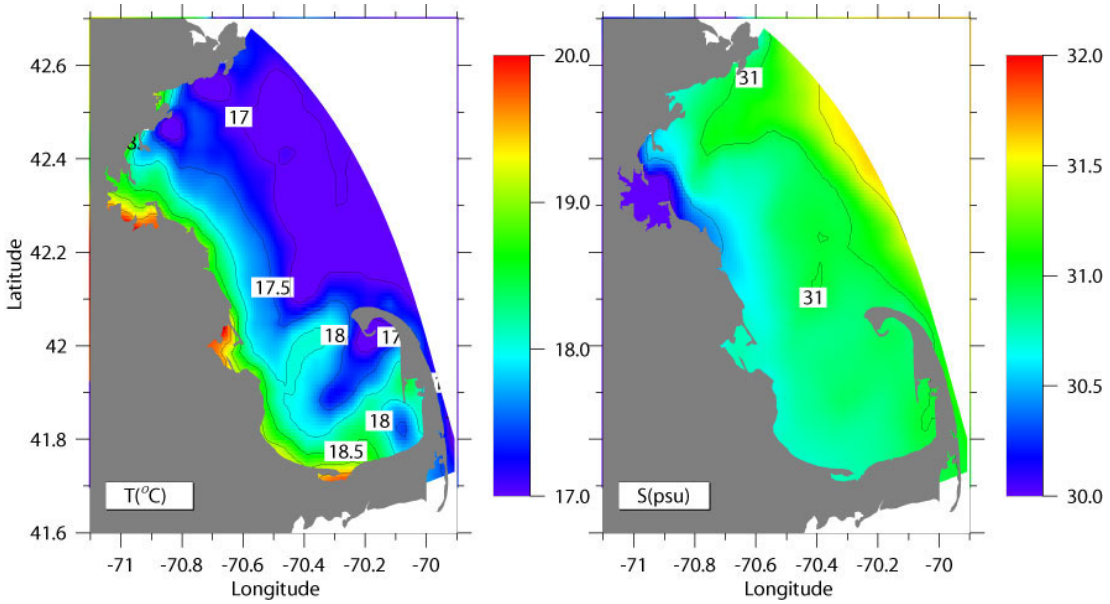

(d)

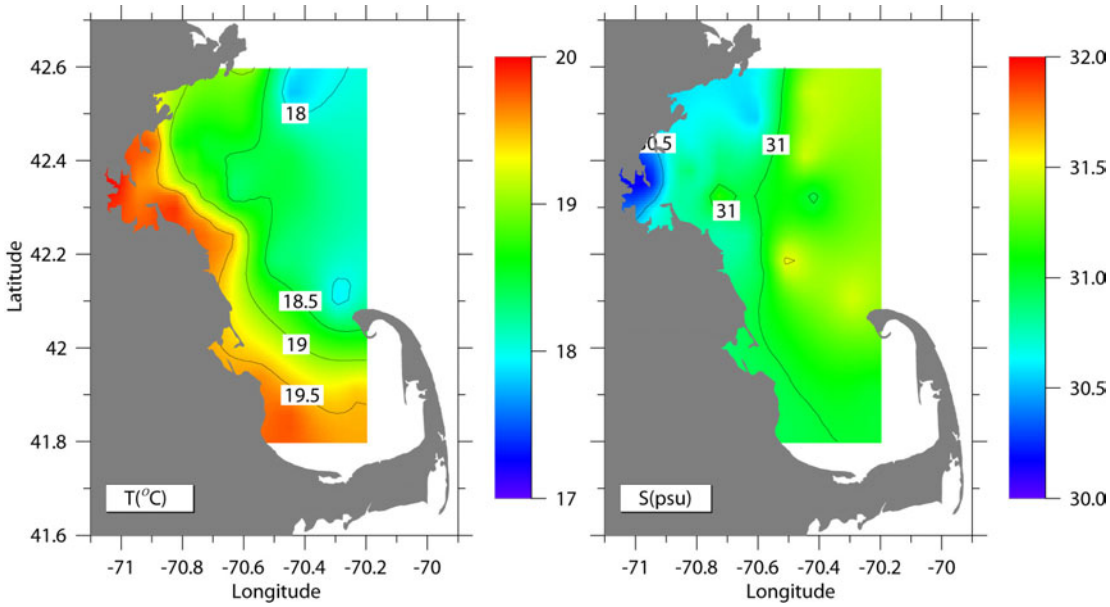

Figure 3.10. Continued.

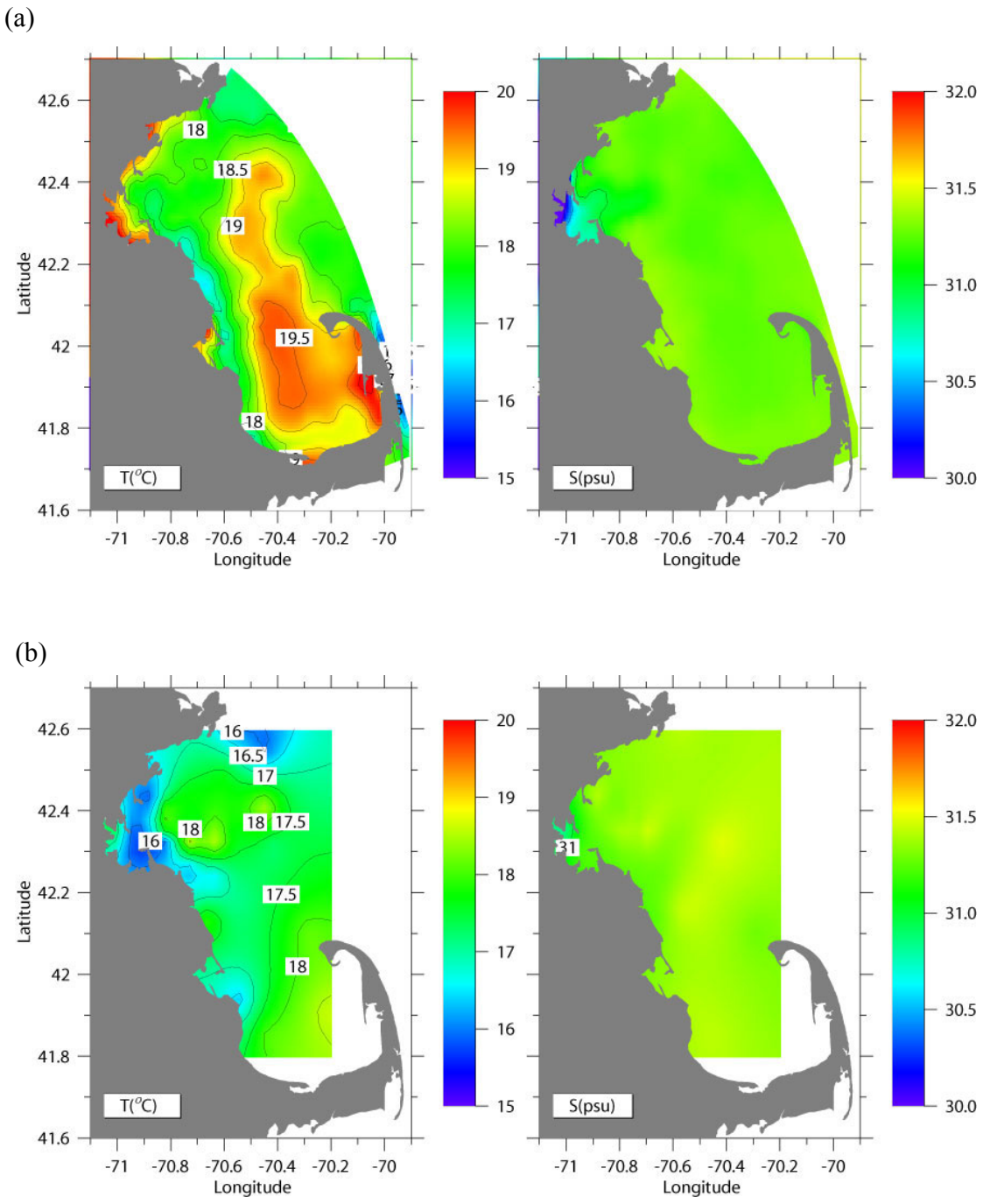

Figure 3.11. Comparisons between modeled and observed surface temperature and salinity for selected cruises in 2001: (a) modeled results on August 27, and (b) observed in August 26-30.

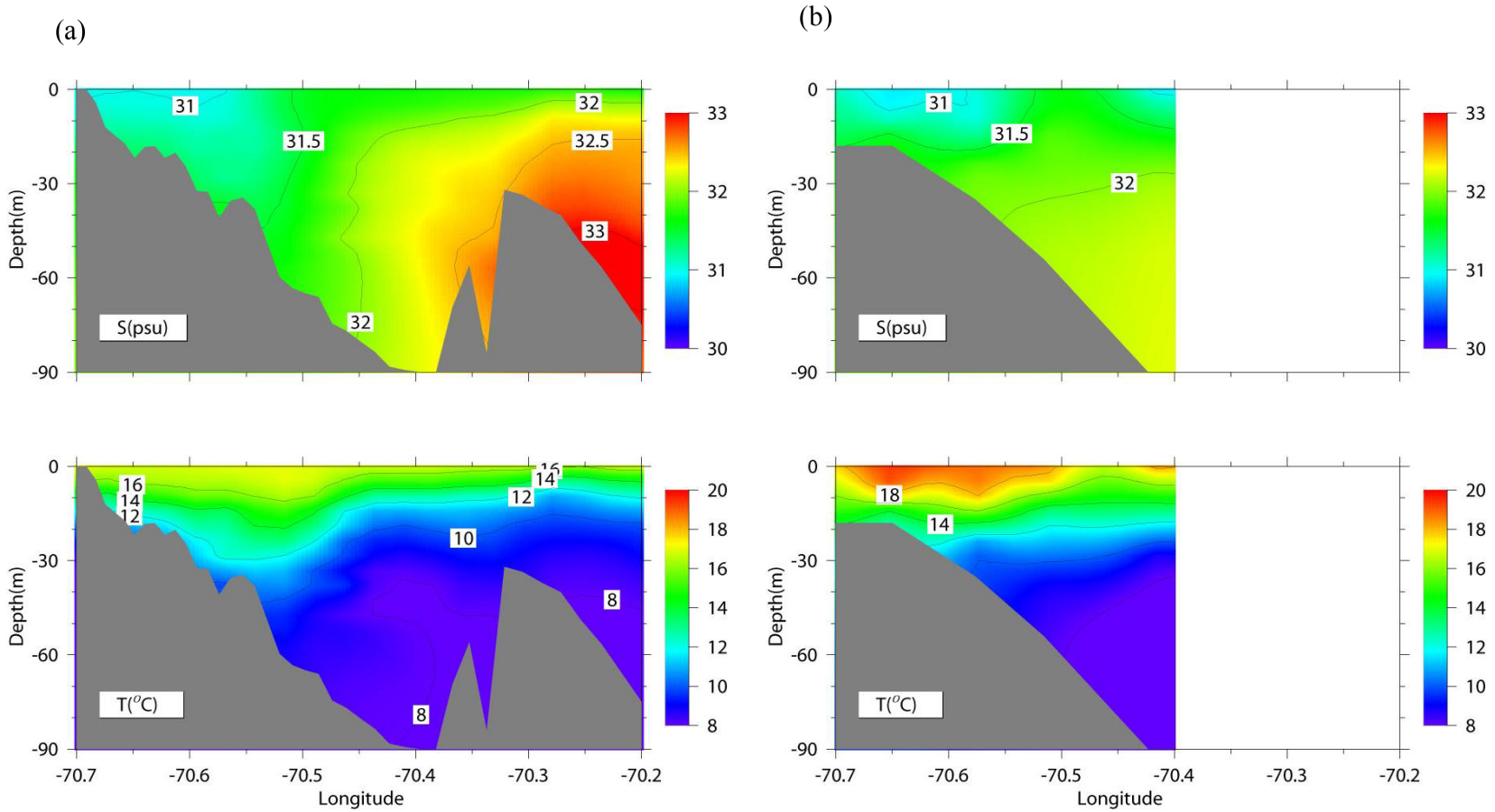

Figure 3.12. Comparisons between modeled and observed temperature and salinity along section 1 from Scituate to Stellwagen in 2000: (a) modeled results on August 17, and (b) observations in August 16-20.

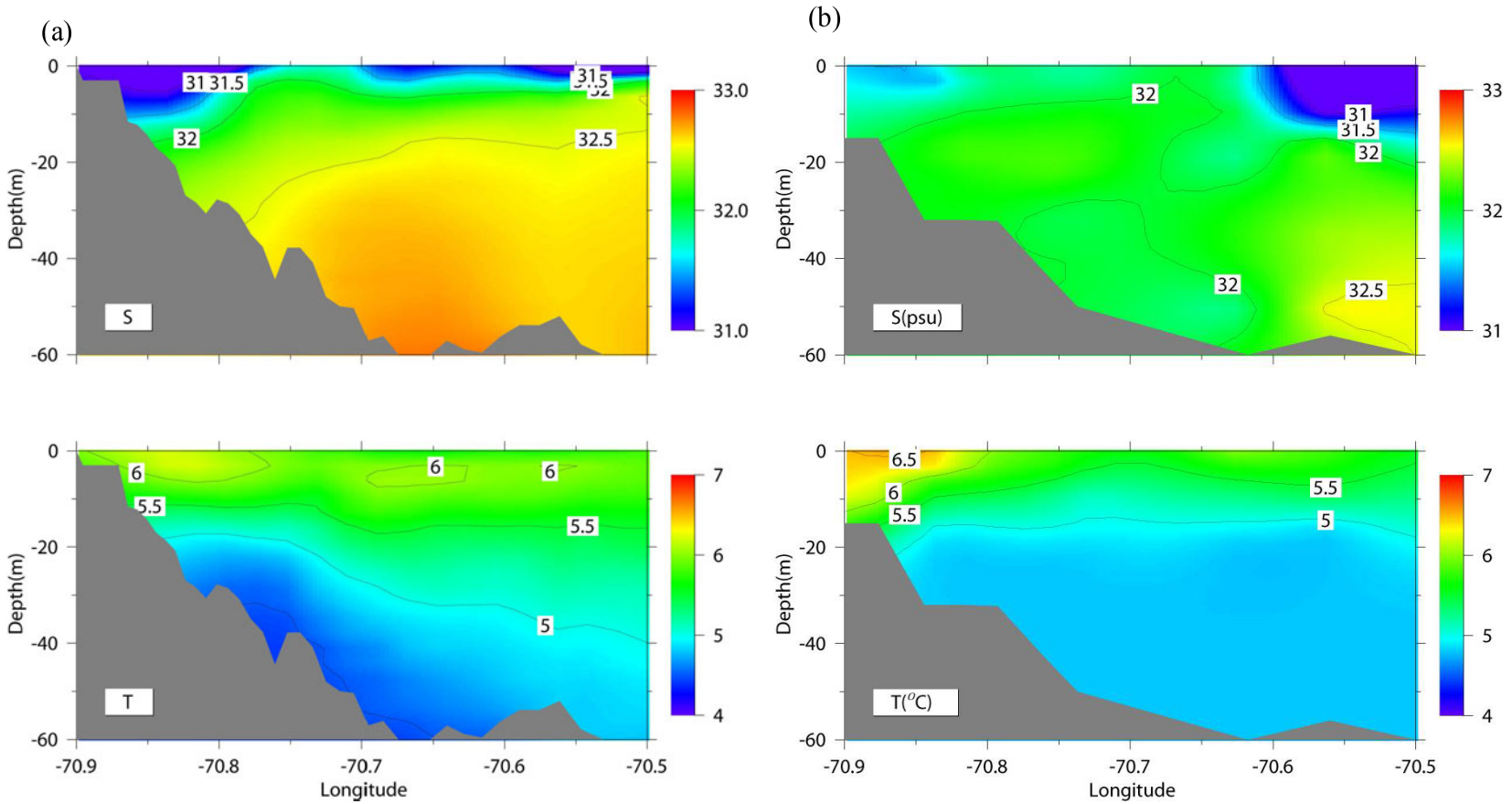

Figure 3.13. Comparisons between modeled and observed temperature and salinity along section 2 from Hull to Cape Ann in 2000: (a) modeled results on April 2, (b) observations in March 31-April 3, (c) modeled results on August 17, (d) observations in August 16-20, (e) modeled results on October 5, and (f) observations in October 3-5. (to be continued on the next page.)

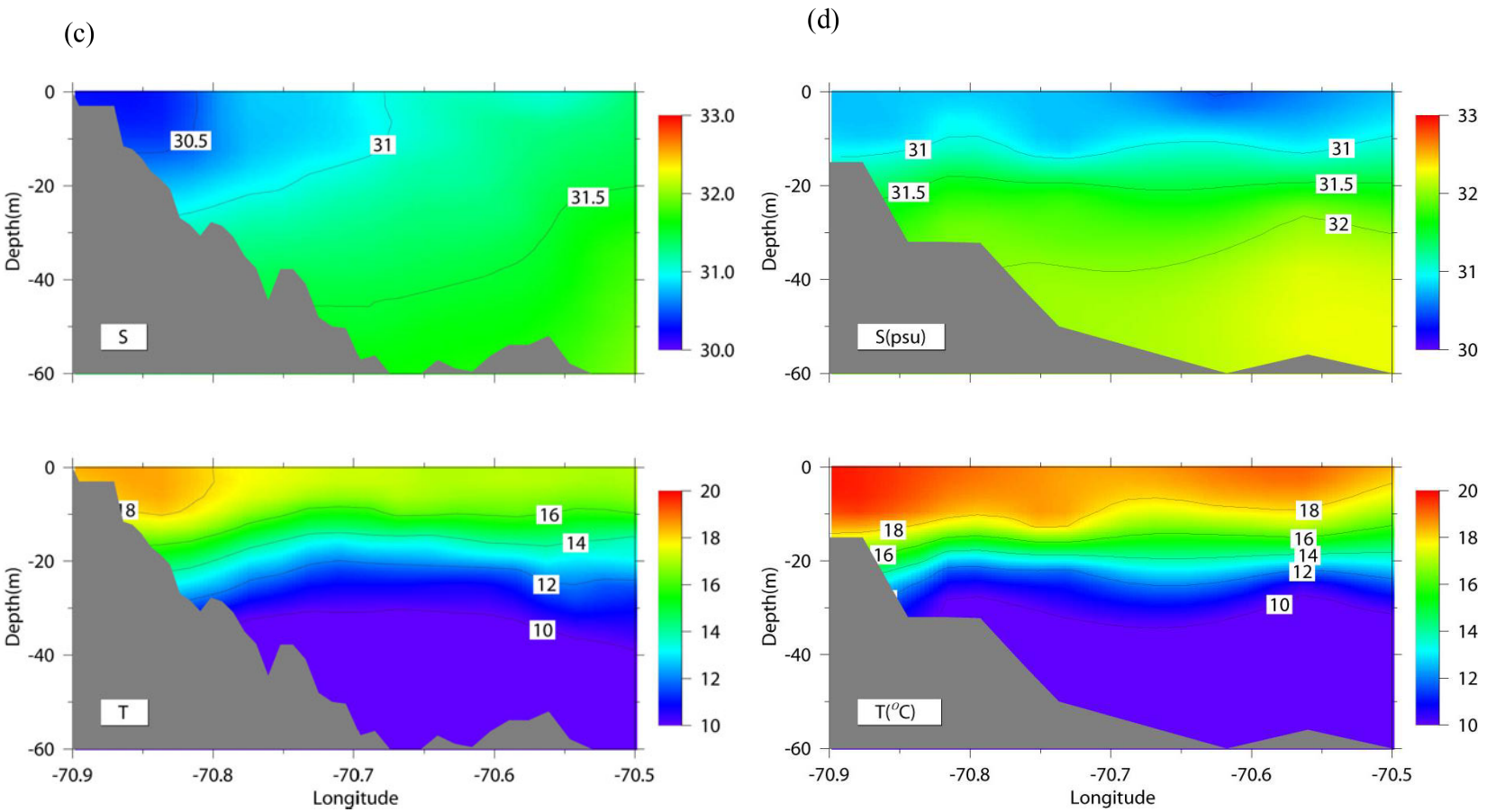

Figure 3.13. Continued.

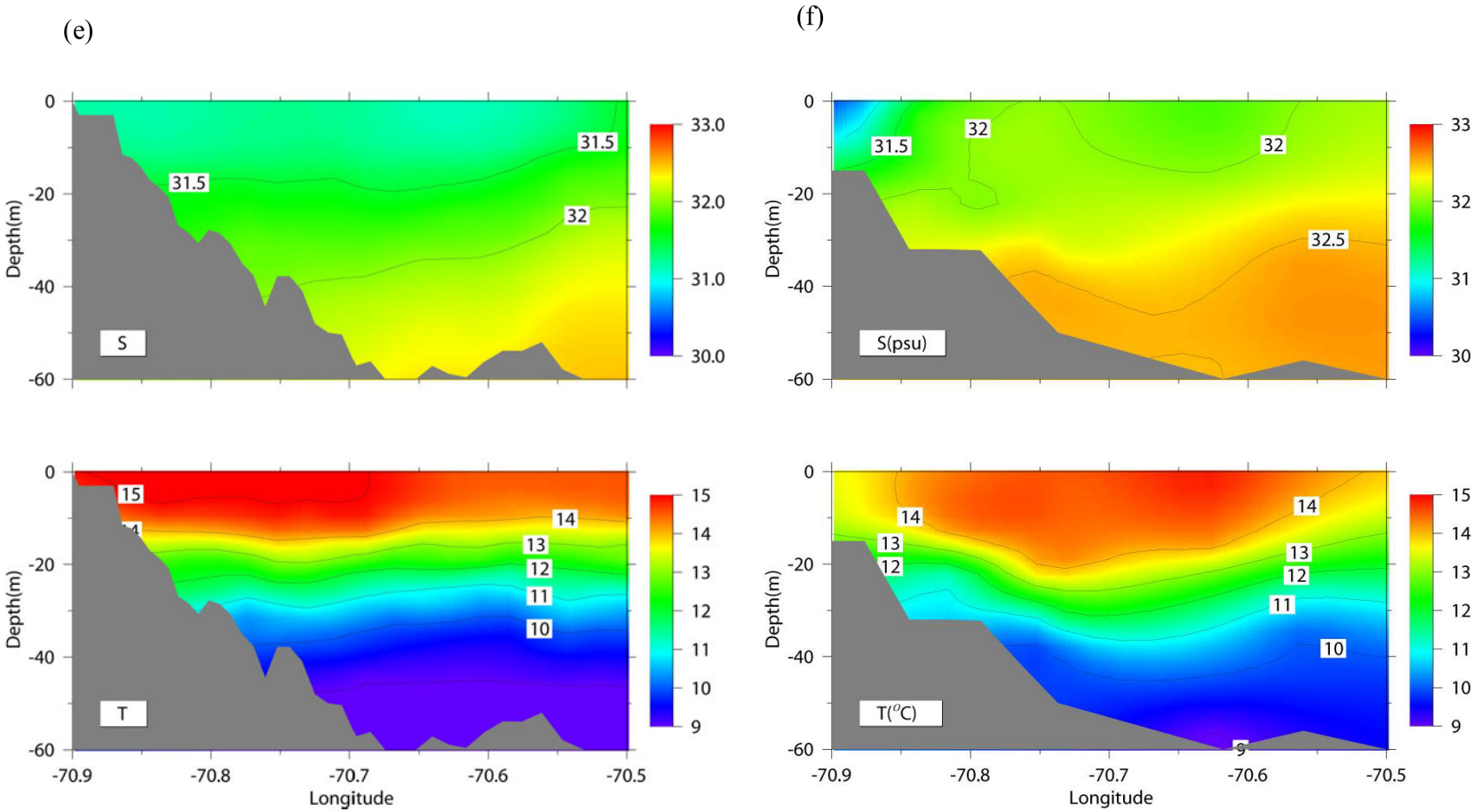

Figure 3.13. Continued.

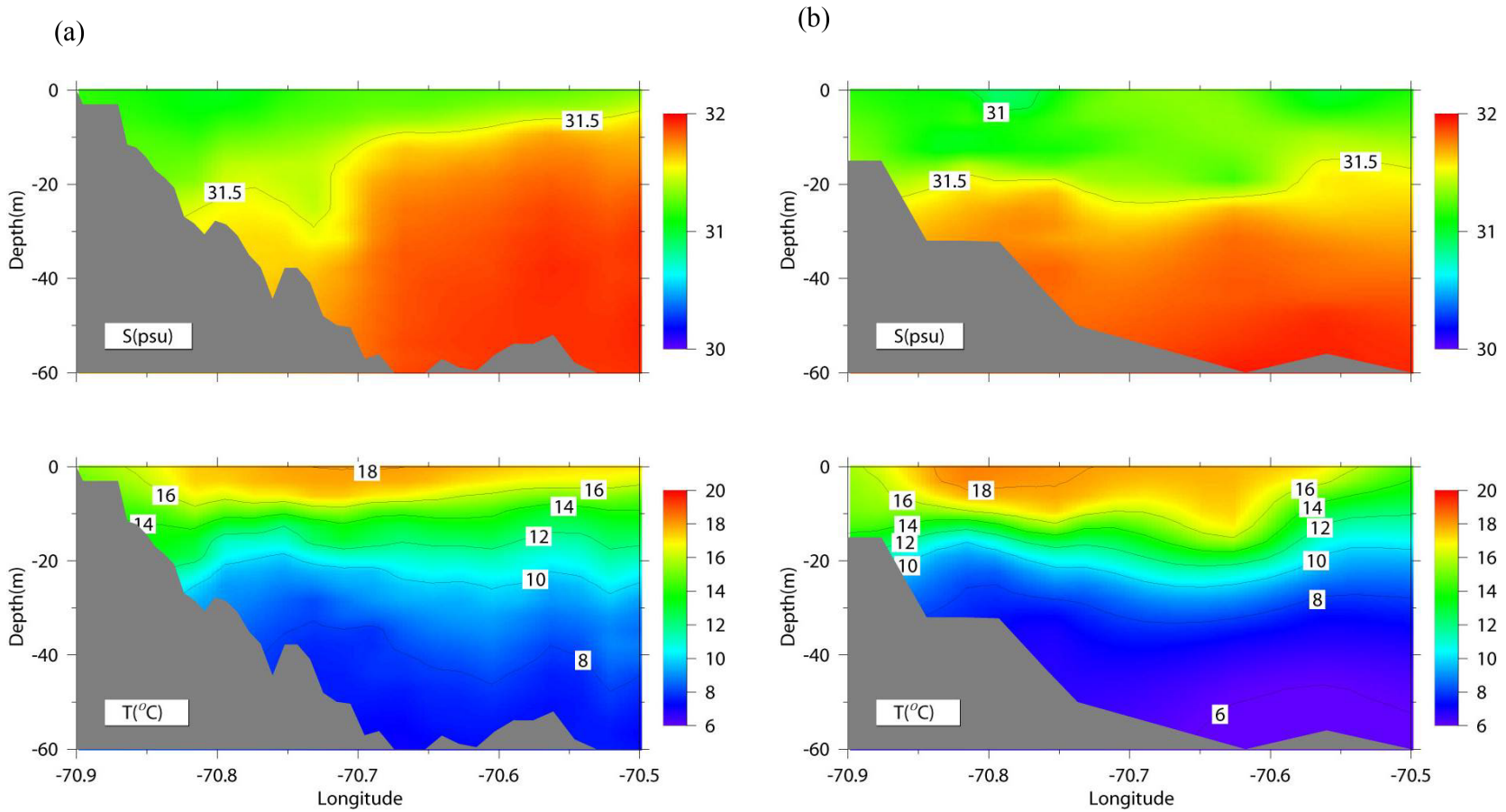

Figure 3.14. Comparisons between modeled and observed temperature and salinity along section 2 from Hull to Cape Ann in 2001: (a) modeled results on August 27, and (b) observations in August 26-30.

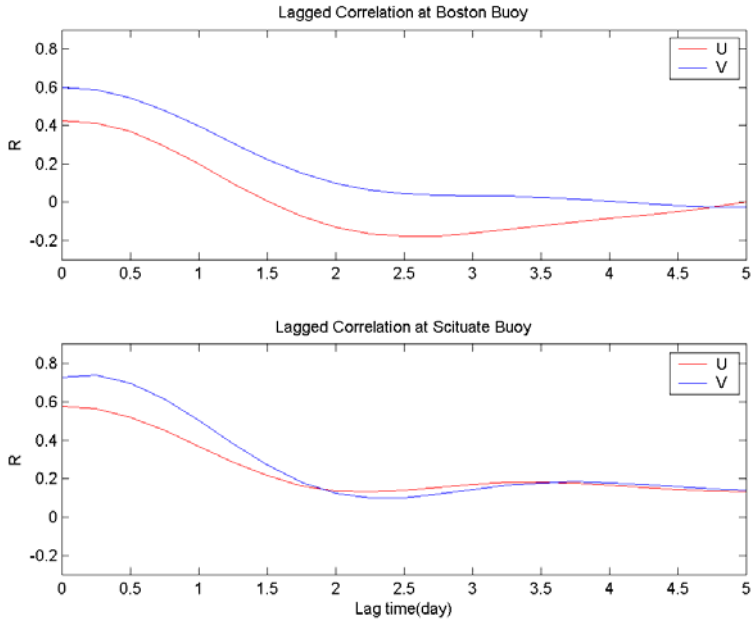

Figure 3.15. Cross-correlation between modeled and observed surface currents at (a) Buoy A and (b) Buoy B in 2000. The currents are filtered with a 60 hour Lanczos filter before correlation calculation.

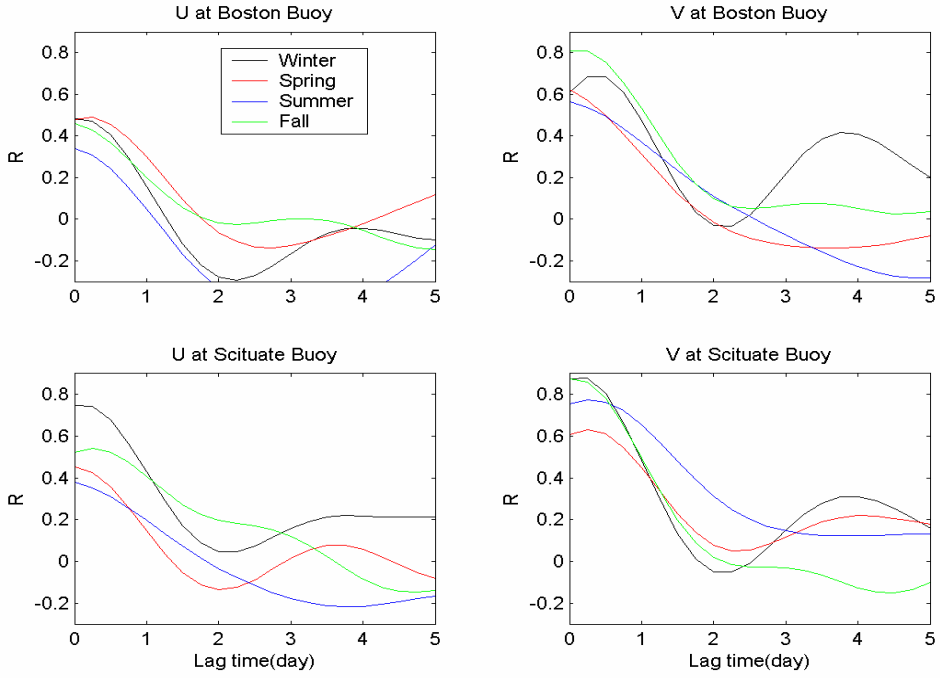

Figure 3.16. Cross-correlation between model and observed surface currents for different seasons in 2000: (a) W-E component at Buoy A, (b) N-S component at Buoy A, (c) W-E component at Buoy B, and (d) N-S component at Buoy B. The currents are filtered with a 60 hour Lanczos filter before correlation calculation.

4. DISCUSSION

4.1 Effects of different open boundary treatments

The procedure that had been used for the 1992-94 and 1998-99 model runs to construct the monthly empirical sea surface elevation (ESSE) along the open boundary requires 1) a direct copy of the monthly sea surface elevation from the previous year, and then 2) a tuning based on the modeler's experience to adjust the sea surface elevation for better fits between the modeled and observed currents at buoys. Such procedures are tedious and subjective, which do not take advantage of all available data. Using the diagnostic sea surface elevation (DSSE) based on the geostrophic balance relation along the open boundary incorporates all observed temperature and salinity data in an objective and best way. Another advantage of this newly developed open boundary treatment is its simplicity, that is, the sea surface elevation at the open boundary is objectively interpolated and computed automatically without a need of subjective tuning. A comparison between the 2000 model results from the ESSE (HydroQual and Signell, 2001) and the new DSSE is made.

The model results based on the DSSE not only resemble the results based on the ESSE, but also are significantly improved in the modeled currents during the summer (Figure 4.1). For example, at Buoy A in August 2000, the surface currents from day 5 to 13 and from day 21 to 30 and the bottom currents from day 14 to 22 based on the DSSE agree better with the observed than the currents based on the ESSE in both magnitude and direction. The modeled currents at Buoy B based on the DSSE are also improved slightly.

The improvements in modeled currents can be further quantified by using correlation analysis (Table 4.1). The correlation between the modeled and observed N-S current component at Buoy A is 0.57 based on the DSSE comparing to 0.45 based on the ESSE. Relatively small improvement is made at Buoy B; the correlation between the modeled and observed E-W current component increases from 0.33 based on the ESSE to 0.38 based on the DSSE. Overall, the correlations between the modeled and observed currents are improved by using the DSSE.

The improvements in the current comparisons based on the DSSE suggest that the diagnostic monthly surface elevations based on objective interpolation and the geostrophic balance relation well represent the low frequency variation in geostrophic currents along the open boundary that

are associated with observed monthly variation in temperature and salinity fields. These monthly variations vary from year to year and are not present in the ESSE. In particular, horizontal gradients of temperature, salinity, surface elevation and currents near the northern boundary are critical upstream conditions for the model. The simulation with the DSSE demonstrates that more observations along the open boundary lead to better model results in the nearfield.

4.2 Seasonal cycle of the MBS circulation

The temperature, salinity and circulation in Massachusetts Bay are strongly driven by the winds (Figure 4.3 and 4.4). Earlier studies have indicated that the seasonal variability of circulation is associated with the seasonal wind patterns (Geyer et al., 1992; Lermusiaux 2001). However, a comprehensive field study of the seasonal variability is difficult and expensive, especially in winter. A numerical model becomes a useful tool to access all seasons after the careful calibration.

The circulation in the winter (December, 1999 and January-February, 2000) in Massachusetts Bay is predominantly southeastward sweeping through the entire bay (Figure 4.1a). The deep GOM water intrusion into Massachusetts Bay is restricted within Stellwagen Basin; the majority of the WMCC flows along the eastern flank of Stellwagen Bank with a magnitude of 20 cm s^{-1}. The currents in Massachusetts Bay are mostly driven by local winds with a current magnitude of 10~15 cm s^{-1}. A stripe of cold water along the southwest coastline is clearly produced by local cooling. The coldest waters are found in Boston Harbor and southeastern Cape Cod Bay due to relatively small heat capacities in shallow waters. The strong vertical and horizontal mixing by winter storms leads to a smooth onshore-offshore gradient in the salinity field with the lowest salinity waters in Boston Harbor and the estuary of the Merrimack River (Figure 4.4a).

The spring (March, April and May) circulation pattern is very similar to the winter circulation pattern in 2000 with relatively weaker currents, particularly on top of Stellwagen Bank (Figure 4.3b). The GOM intrusion is the strongest among 4 seasons; it flows along the western coast and penetrates deeply into Cape Cod Bay. The temperature field is uniformly distributed over the entire region except in Boston Harbor and the southeast portion of Cape Cod Bay where the warmest waters are found, owing to the spring surface heating. The salinity field shows low salinity waters off Cape Ann and near Boston Harbor influenced by the local freshwater runoff (Figure 4.4b). Overall, the winter-spring circulation patterns represent the

conventional view of the circulation in Massachusetts Bay (Geyer et al., 1992).

By contrast, the summer circulation shows a dramatically different pattern from those in winter and spring (Figure 4.3c). While the WMCC is strong and remains on the eastern flank of Stellwagen Bank, the intruding current is very weak, but clearly present. The coastal currents are northward in western Massachusetts Bay. The fresh water from Boston Harbor is pushed northeastward, and then flows southeastward along the western flank of Stellwagen Basin toward the South Passage exiting Massachusetts Bay. A weak anti-cyclonic eddy consisting of average 19°C warm water occupies entire Cape Cod Bay. The warm water flows northeastward and joins the outgoing flow in the South Passage. The summer salinity is the lowest among 4 seasons in Massachusetts Bay. The plume of low salinity water extends from Boston Harbor well into the bay.

In the fall, the WMCC is still mainly restricted on the eastern flank of Stellwagen Bank, bypassing Massachusetts Bay (Figure 4.3d). Along the northern coast the coastal currents flow northeastward joining the WMCC. Near Boston Harbor, the fresh water plume turns southward and joins the southward coastal current flowing along the west coast into Cape Cod Bay. The horizontal north-south temperature gradient still exists with cold water near the north shore and warm water in Cape Cod Bay, but is much reduced compared to the summer temperature gradient.

The seasonal variability in the circulation patterns determines the water exchange between Massachusetts Bay and the GOM. The intrusion of the GOM water into Massachusetts Bay varies, being mostly restricted to Stellwagen Basin in the winter, intruding deeply into the western coast and Cape Cod Bay in the spring, and bypassing Massachusetts Bay through the eastern flank of Stellwagen Bank in summer and fall. Such seasonal variation of the circulation in Massachusetts Bay will not only affect the seasonal nutrient fluxes between GOM and the MBS, but also the seasonal biota transport and accumulation in Massachusetts and Cape Cod Bays.

4.3 The MBS responses to wind variability in summer

The bottom water renewal in Stellwagen Basin is important to the fate of organic matter and the water quality, especially in summer when organic matter formed during the spring bloom settles down to the deep water and is decomposed. The decomposition process consumes

dissolved oxygen. Though the seasonal circulation pattern shows the restriction of the GOM water into Massachusetts Bay, low frequency wind events can lead to significant variability in both the surface and deep water renewals. The wind changes its direction and magnitude every 5-10 days as measured at the Boston Buoy during the summer (Figure 4.4), which is typical of synoptic processes. The currents in Massachusetts Bay respond as typical coastal upwelling or downwelling scenarios: a northerly wind drives an onshore Ekman transport and downwelling as well as a southward geostrophic coastal current; and a southerly wind drives an offshore transport and upwelling as well as a northward geostrophic coastal current. To compensate the onshore and offshore Ekman transport, deep water circulations are induced.

Examples of the coastal responses to wind forcing are shown in Figures 4.5 and 4.6. The modeled temperature and salinity at the Scituate buoy station in August 2000 are consistent with the observed in response to the wind forcing. The water is weakly stratified at the beginning of August, which is due to earlier wind mixing. The thermocline and halocline are uplifted and intersect the surface in response to the southwesterly-wind-induced Ekman pumping. Though the wind has changed its direction to a downwelling favorable wind on day 9, the uplifted thermocline and halocline remain until day 12. The downwelling favorable wind lasts approximately a week with a peak at day 15. The thermocline and halocline are depressed by the downwelling and the mixed layer depth reaches approximately 12 m. During the relaxation period, the upper water column is restratified again. On day 21, the wind becomes southerly. The thermocline and halocline are uplifted again by the upwelling.

Two horizontal snapshots of the surface and near bottom currents in Massachusetts Bay on day 15 and day 25, respectively, elucidate the circulation fields associated with strong northerly and southerly winds (Figures 4.7 and 4.8). On day 15, the surface currents in Massachusetts Bay are mostly southward and southwestward with intrusion of the GOM water into Massachusetts Bay under a northerly wind prior to day 15. In association with the warm water pooled in the western coastal area, the strong coastal current penetrates deeply into western Cape Cod Bay without any surface return currents. In eastern Cape Cod Bay, upwelling can be identified from the low temperature along with meandering features at scales from 10 to 20 km. At the southern end of Stellwagen Basin, upwelling is relatively weak, while there is an intensified intruding current through the South Passage off Race Point. Such upwelling phenomena have been observed during a northeasterly wind event in late September, 1998 (Yu et al., 2002). After the

wind becomes southerly on day 21, a strong northward coastal jet has developed on day 25 extending from Cape Cod Bay to the Merrimack River along the upwelling front, as indicated by the temperature gradient from 16ºC in near shore areas to 17.5ºC in offshore areas. The coastal current exits Massachusetts Bay through the North Passage, and bifurcates into two branches. The northern branch goes around Cape Ann and continues northward, and the southern branch turns southward to join the WMCC. The surface water in Massachusetts Bay also exits through the South Passage. As a consequence, the GOM water is restricted to the east of Stellwagen Bank. An anticyclonic eddy of relatively warm water is formed in Cape Cod Bay.

The near bottom circulation patterns at 50m in Stellwagen Basin on days 15 and 25 show very different patterns: little horizontal exchange between Stellwagen Basin and the GOM are found on day 15, and a strong intrusion of the GOM water into Stellwagen Basin is found in the North Passage with a current speed of 5-6 cm s^{-1} on day 25 (Figure 4.8). A narrow jet of the intruding GOM water starts from the deep basin north of Stellwagen Bank, flows northward along the shallow flank, turns westward into Stellwagen Basin, and forms a southward jet in a confined 8 km band crossing the basin and penetrating into Cape Cod Bay. This jet appears to be separated from the WMCC, and is originated from the deep basin next to the northeastern flank of Stellwagen Bank.

The interaction between the Ekman transport, stratification and bottom topography determines vertical circulation patterns in Massachusetts Bay. On day 15, the onshore Ekman transport produces the downwelling along both the western coast of Massachusetts Bay and the eastern flank of Stellwagen Bank (Figure 4.9). An upwelling occurs in the middle of Stellwagen Basin and forms a circulation cell over the western slope of the basin together with the downwelling near the coast. A similar circulation cell is also found on the eastern flank of Stellwagen Bank. In western Massachusetts Bay, the warm surface water accumulates with weak stratification in the area shallower than the 20 m isobath (Figure 4.7a). On day 25, the southerly wind drives an offshore Ekman transport and strong upwelling near the western coast, and produces a coastal upwelling front. The compensation flow is found approximately between 10 and 40 m instead of near the bottom. As the compensation flow reaches the coast, it bifurcates forming two (surface and bottom) circulation cells.

The offshore Ekman transport drives the deep intruding current that compensates the

upwelling in the western coast. A monthly average of bottom currents shows a deep jet similar to that on day 25 (not shown). Estimating Ekman transport under an average upwelling wind condition yields a time scale of approximately 10 days for renewing the bottom water (Jiang and Zhou, 2003). Thus, the low frequency wind events can produce significant surface and bottom water exchanges between Massachusetts Bay and the GOM, and in turn affect the transport of biota and biochemical processes.

The spin-up time scale can also be estimated at approximately 2-6 days based on the Ekman transport theory (Bowden, 1983). A correlation analysis by Geyer et al. (1992) found a 4 day time-lag between winds in Cape Cod Bay and surface currents measured at Broad Sound, which is close to new outfall site.

Table 4.1 Correlation coefficients between modeled and observed surface currents in summer, 2000 by using ESSE and DSSE

	DSSE	ESSE
W-E velocity at Buoy A	0.34	0.36
N-S velocity at Buoy A	0.57	0.45
W-E velocity at Buoy B	0.38	0.33
N-S velocity at Buoy B	0.75	0.73

(a)

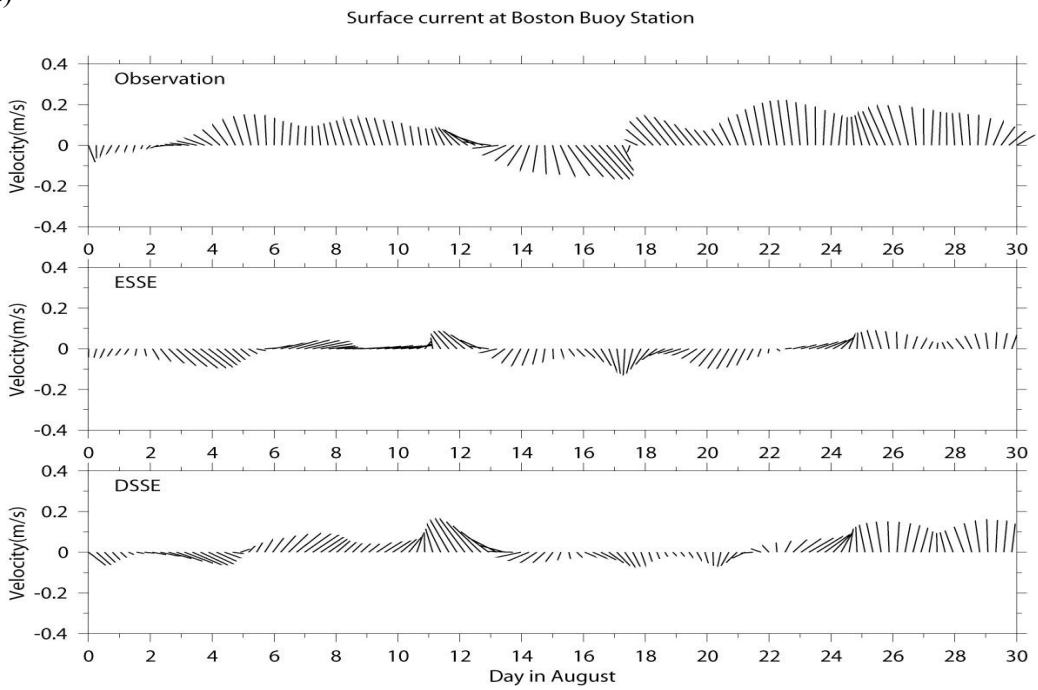

(b)

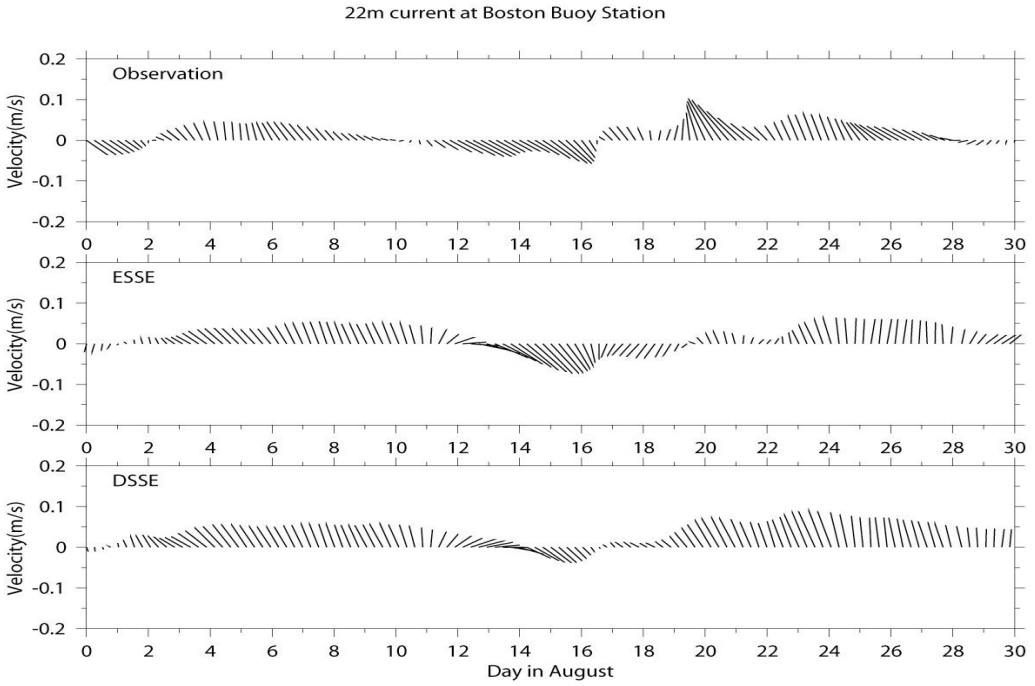

Figure 4.1. Comparisons of modeled currents between using the empirical sea surface elevation (ESSE) and diagnostic sea surface elevation (DSSE) at Buoy A at (a) the surface and (b) bottom in August 2000. The currents are filtered with a 60 hour Lanczos filter.

(a)

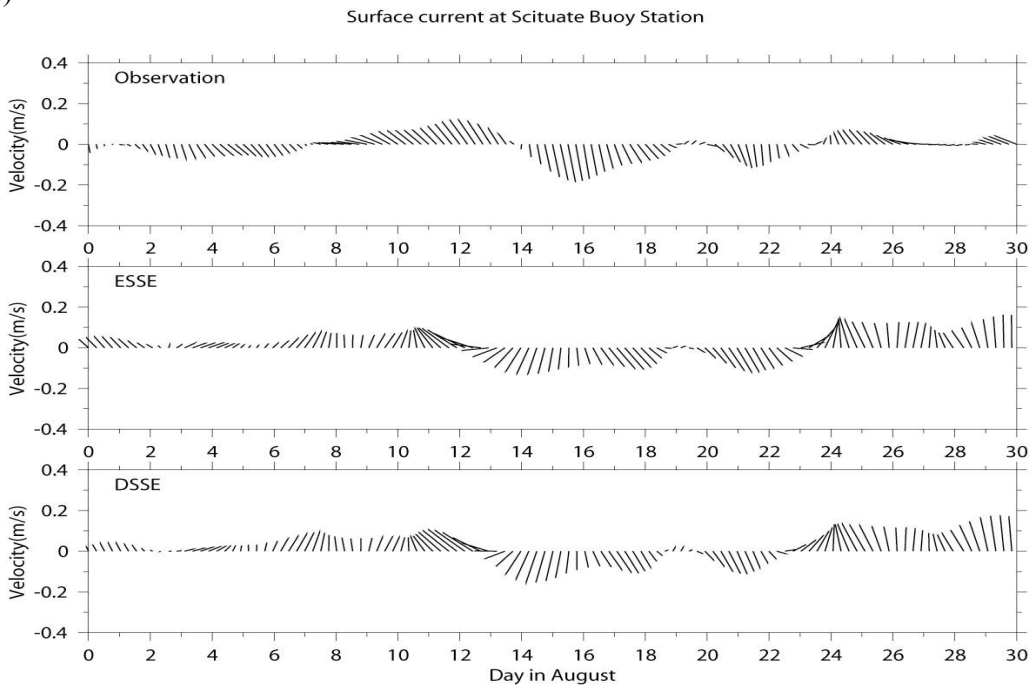

(b)

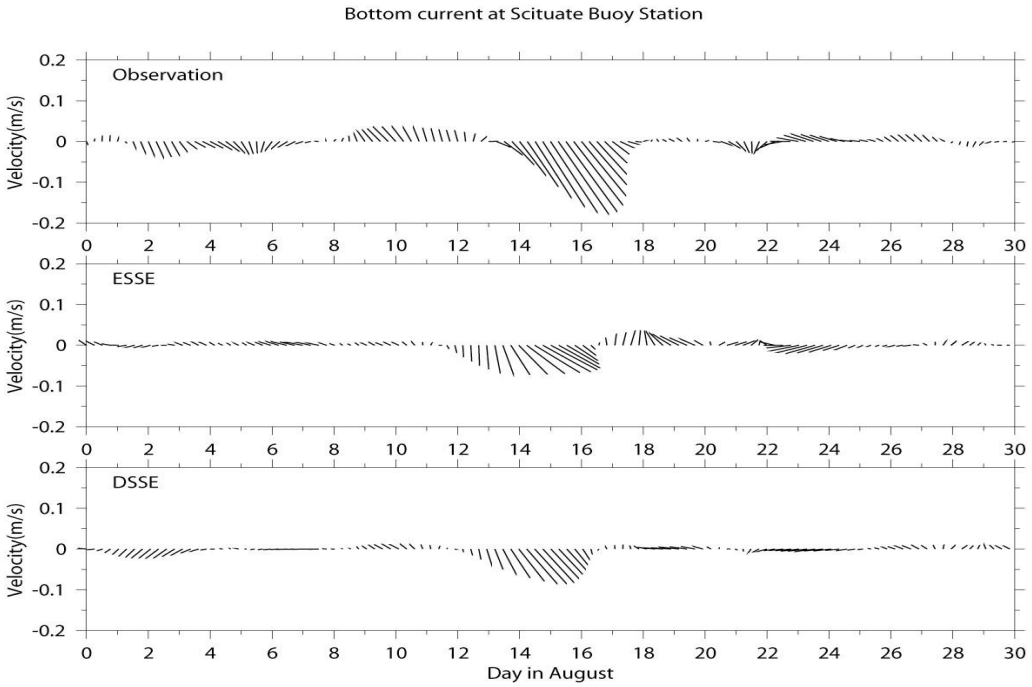

Figure 4.2. Comparisons of modeled currents between using the ESSE and DSSE at Buoy B at (a) the surface and (b) bottom in August 2000. The currents are filtered with a 60 hour Lanczos filter.

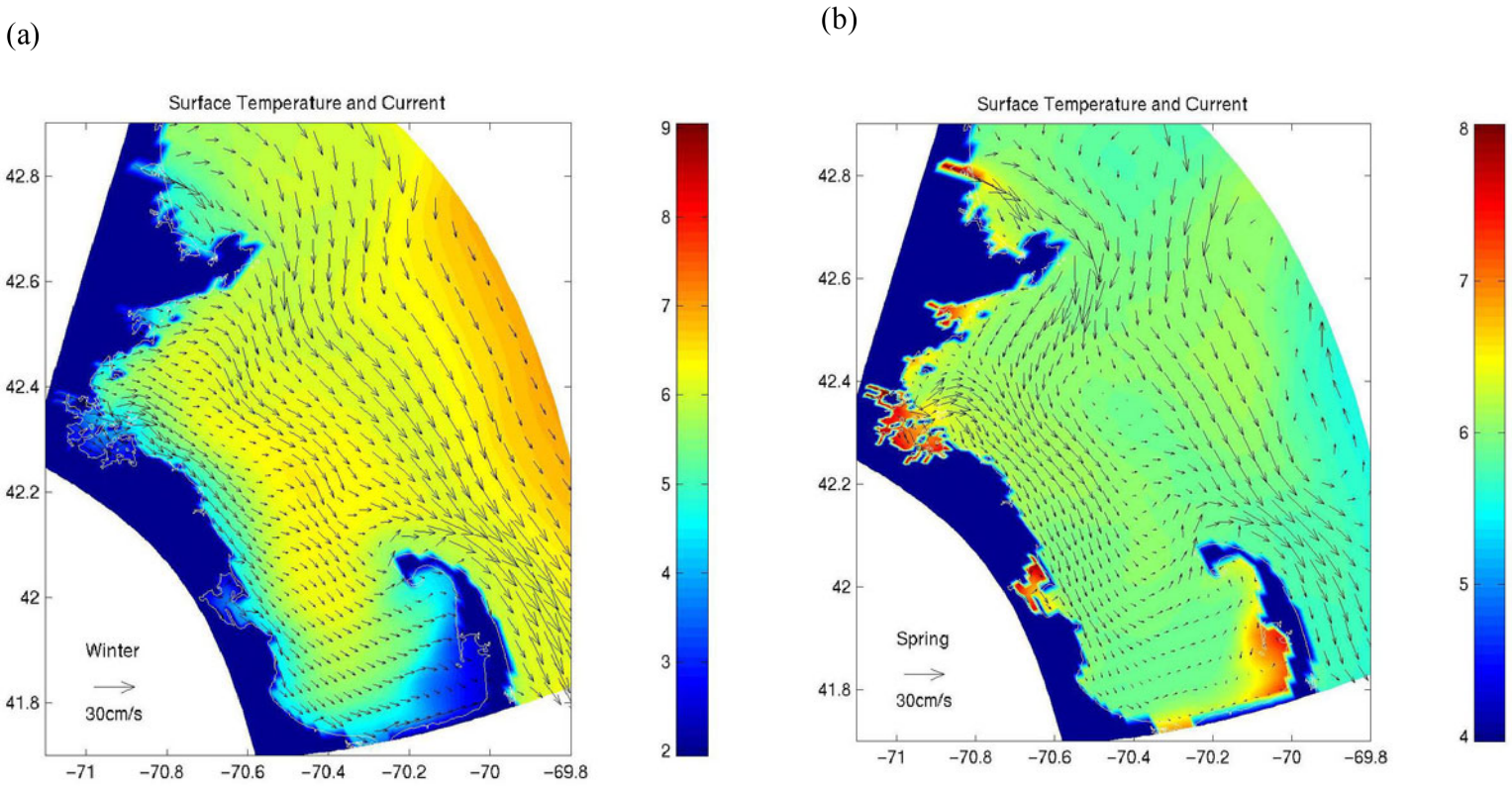

Figure 4.3. Modeled seasonal surface currents and temperature in 2000: (a) in winter from December 1999 to February 2000, (b) in spring from March to May 2000), (c) in summer from June and August 2000, and (d) in autumn from September to November 2000. (to be continued on next page)

(c)

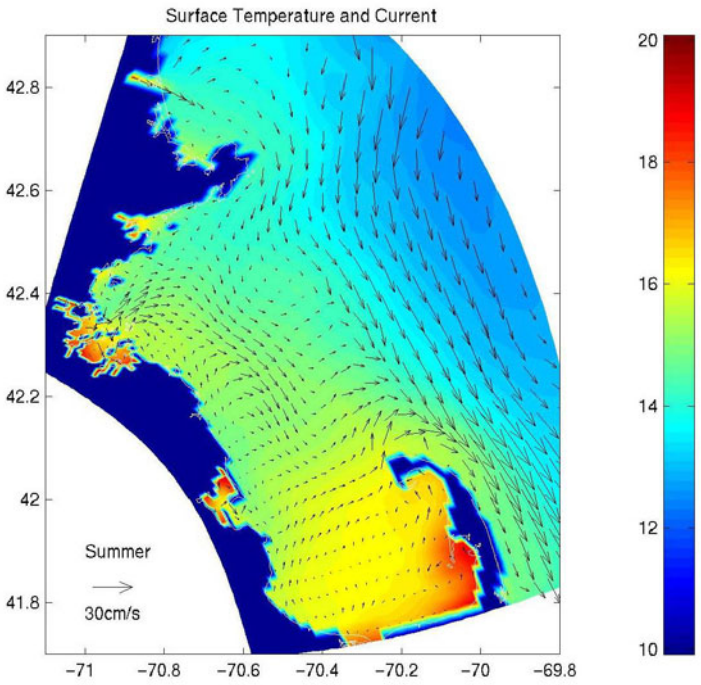

(d)

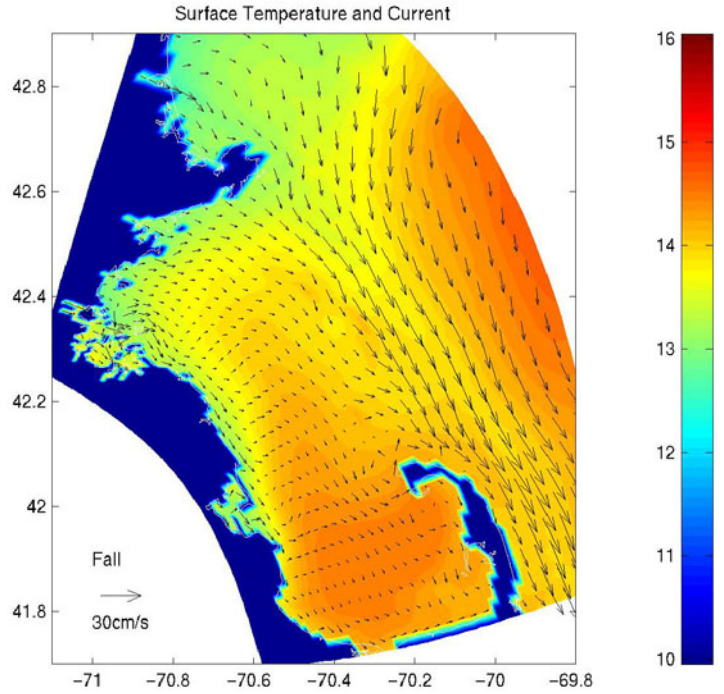

Figure 4.3. Continued.

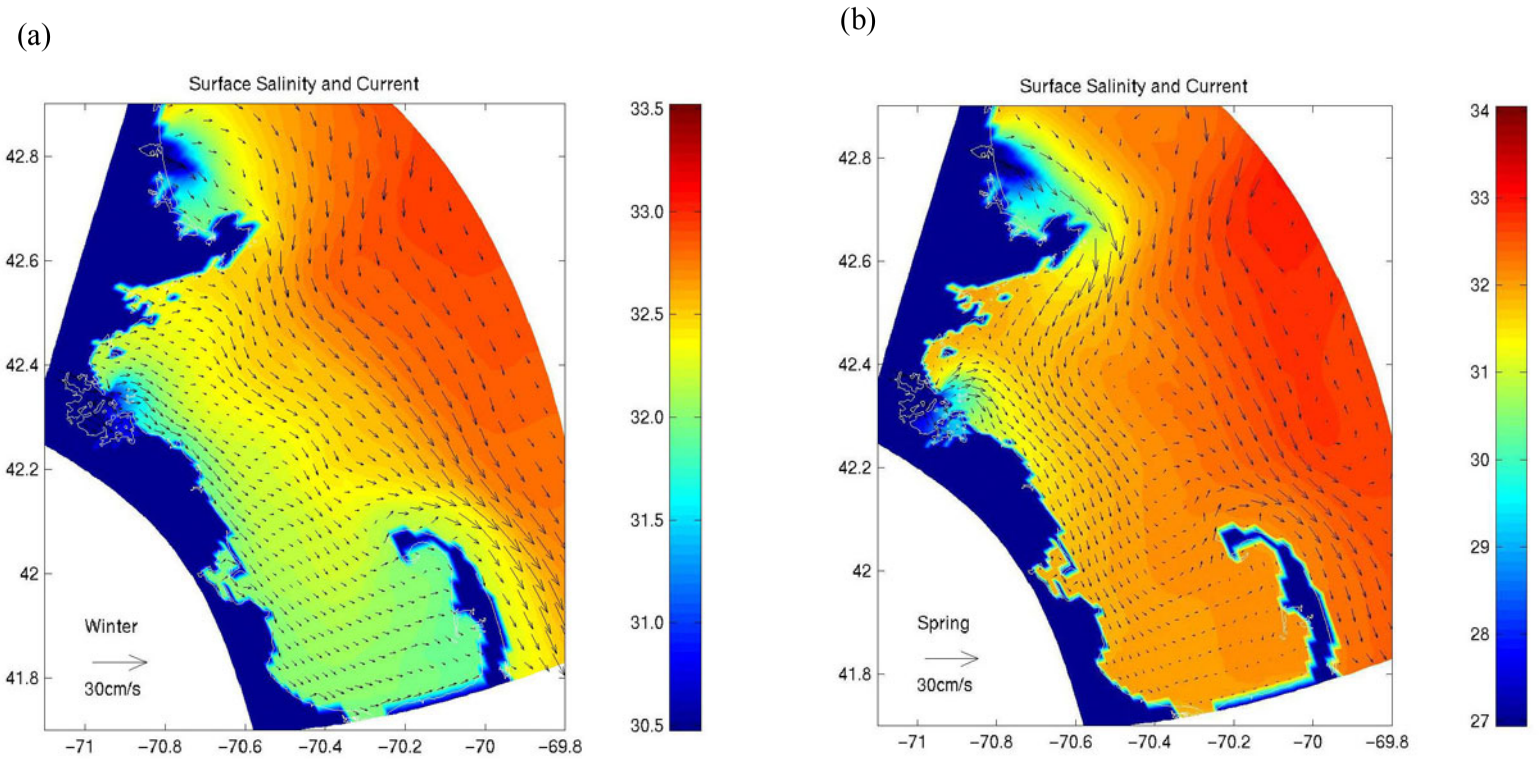

Figure 4.4. Modeled seasonal surface currents and salinity in 2000: (a) in winter from December 1999 to February 2000, (b) in spring from March to May 2000), (c) in summer from June and August 2000, and (d) in autumn from September to November 2000. (continued on next page)

(c)

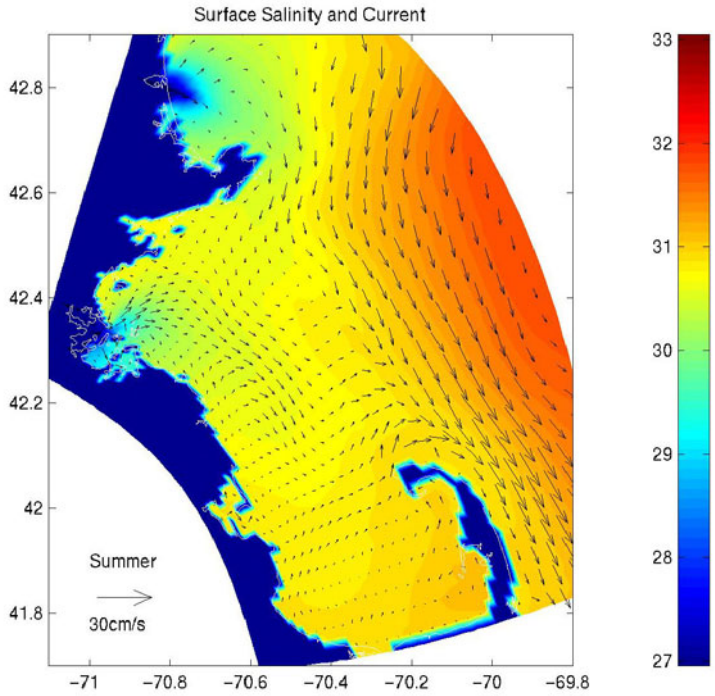

(d)

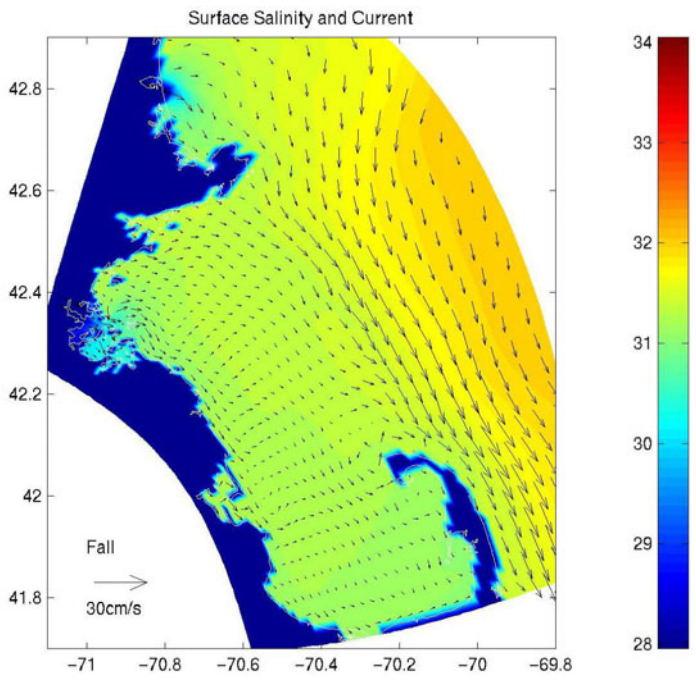

Figure 4.4. Continued.

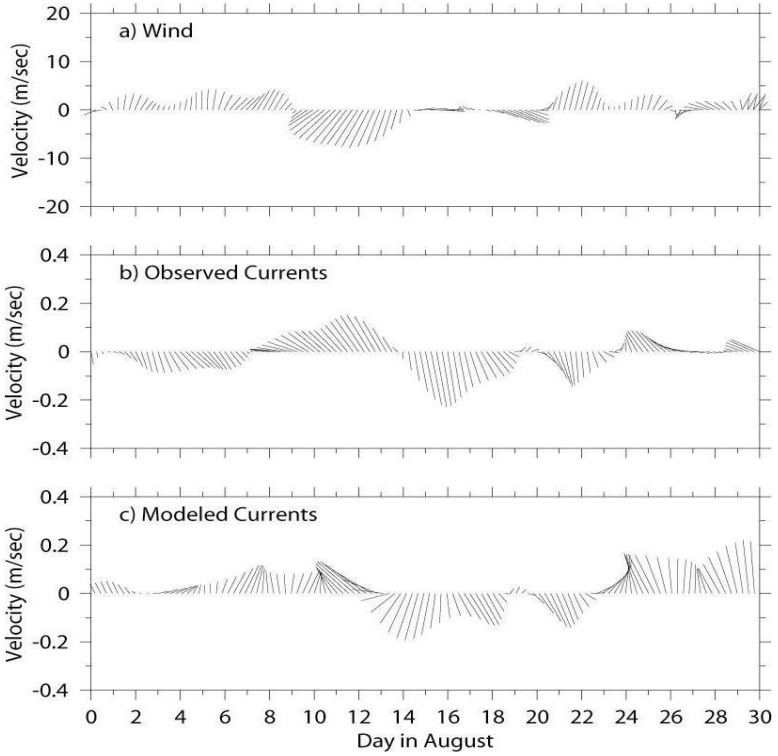

Figure 4.5. Modeled surface currents and observed wind and surface currents at Buoy B in August, 2000. Both wind and currents are filtered with a 60 hour Lanczos filter.

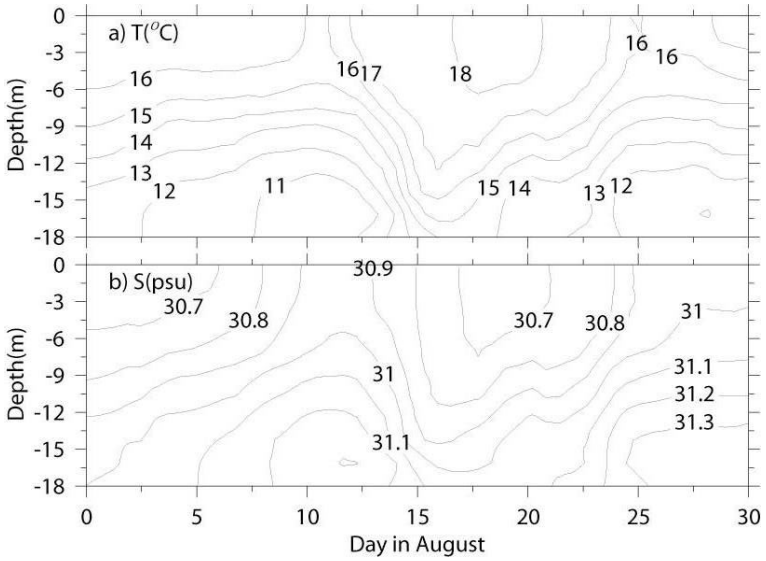

Figure 4.6. Modeled time series of temperature and salinity vertical distributions at Buoy B in August, 2000.

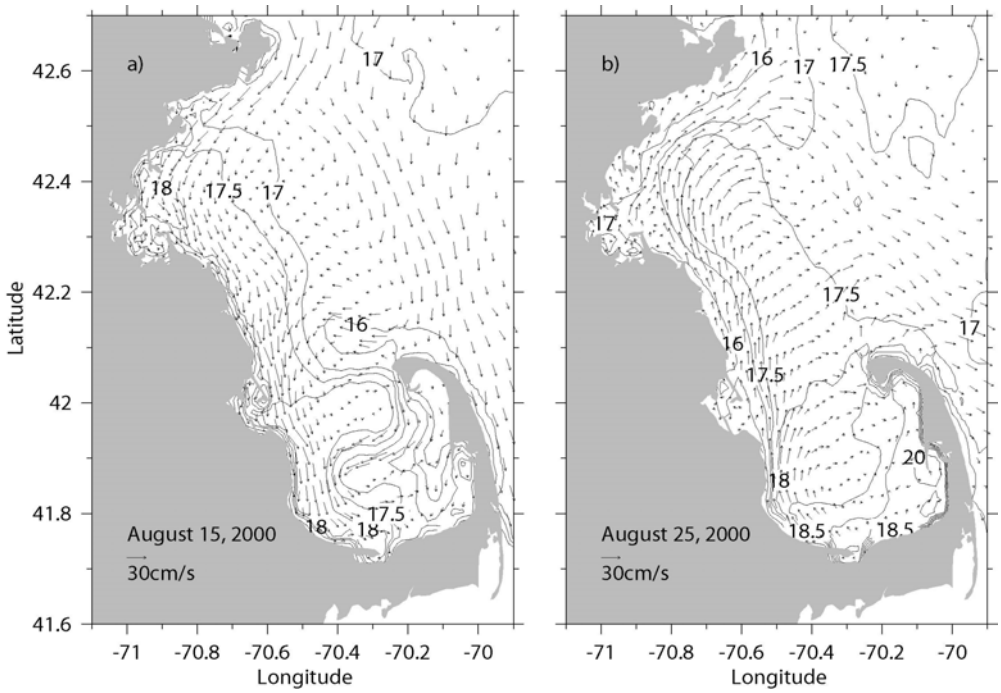

Figure 4.7. Surface temperature and currents on (a) August 15, 2000 and (b) August 25, 2000.

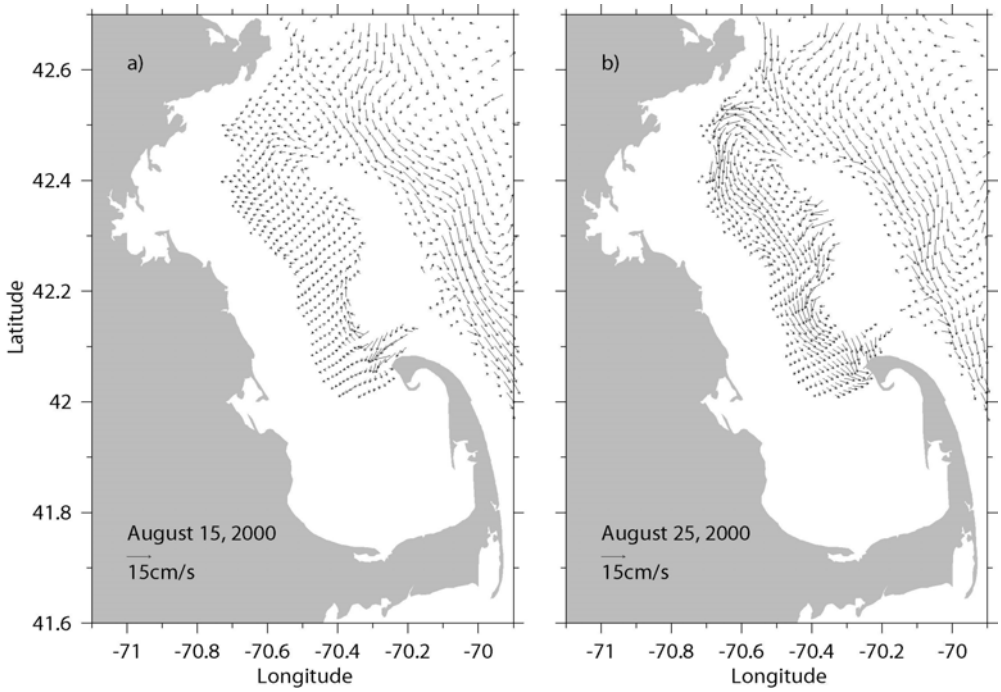

Figure 4.8. Bottom (50m) currents on (a) August 15, 2000 and (b) August 25, 2000.

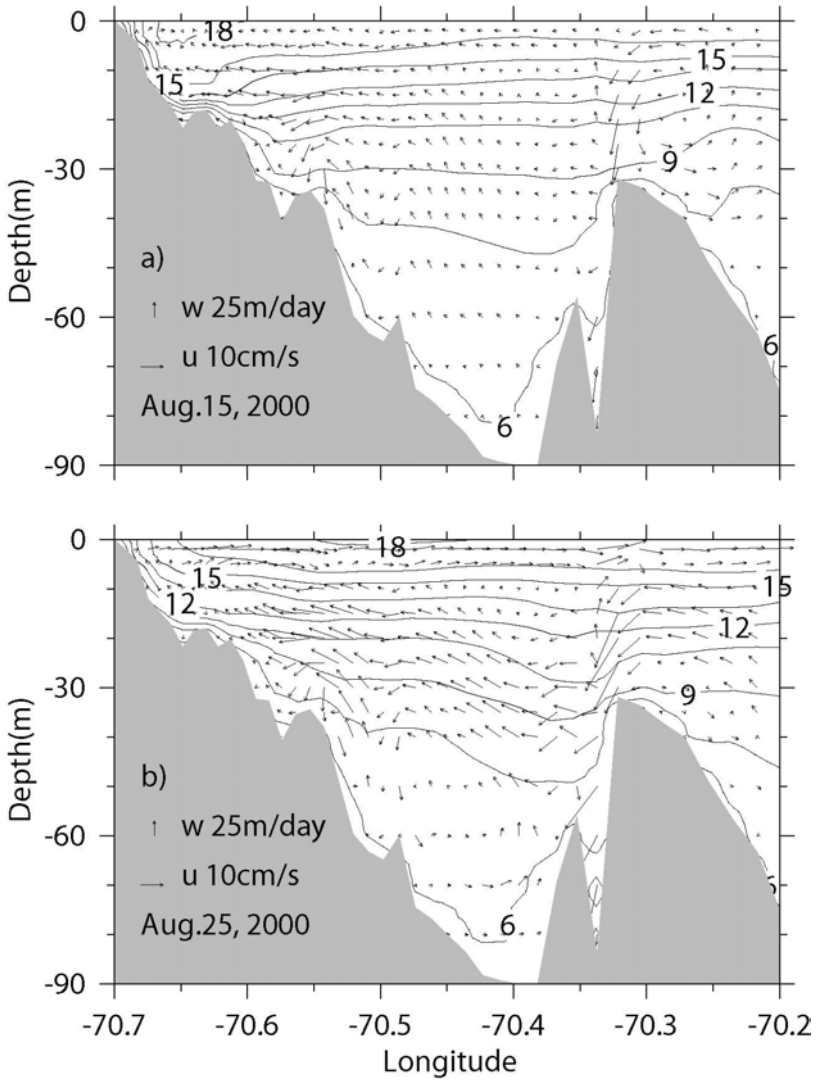

Figure 4.9. Temperature and currents along section 1 from Scituate to Stellwagen Bank on (a) August 15, 2000 and (b) August 25, 2000.

5. SUMMARY AND RECOMMENDATIONS

5.1 Summary

This report presents the calibration and results of the MBS hydrodynamic model runs for years 2000 and 2001. Overall, the modeled seasonal stratification, mixing and circulation patterns compare well to the observed ones in response to seasonal changes in heat fluxes, freshwater inputs and boundary forcing. The modeled spatial and temporal distributions of temperature, salinity and current fields also respond to short term wind events, which produce upwelling and downwelling.

The discrepancies between model results and observation are: (1) the low cross correlation between observed and modeled currents at Buoy B during stratified months, which may be produced by uncertain modeled locations of coastal fronts associated with summer upwelling or downwelling events; and (2) the underestimation of salinity in the nearfield during summer and fall seasons, which may be associated with the GOM water intrusion. To resolve the first discrepancy, more field process studies would be required for resolving upwelling processes, such as upwelling velocities, secondary circulations and frontal locations so that we can diagnose the causes. To resolve the second discrepancy, more spatial and temporal coverage near the open boundary would be needed, especially during summer.

The report also includes the improvement in the procedures constructing open boundary conditions. In the simulation for year 2000, the boundary sea surface elevation is constructed from the geostrophic balance based on objectively interpolated temperature and salinity along the boundary. This method significantly improves the modeled currents in the nearfield during summer, as compared to the method used in previous simulations (HydroQual and Signell, 2001). Model results suggest that the boundary conditions along the northern open boundary are important.

The simulations for years 2000 and 2001 suggest that the summer circulation in the bay strongly responds local wind forcing, which causes inshore/offshore Ekman transports, upwelling and downwelling, strong coastal jets and water exchange between the GOM and Massachusetts Bay. The offshore Ekman transport favors strong bottom water intrusion, which is critical to renewal of the bottom water in Stellwagen Basin.

5.2 Recommendations

Improving the open boundary conditions. Reliable open boundary conditions are critical to the success of model simulations in the MBS. Similar to that suggested by HydroQual and Signell (2001), we also recommend an increase in the number of sampling stations along the open boundary. Particularly in the northern portion of the open boundary, the surface slope and water properties determine the GOM water intrusion into the MBS and ultimately the water properties in the MBS. Since August, 2001, two operational buoys as part of the Gulf of Maine Ocean Observing System (GoMOOS) have been deployed near the northern open boundary and in the North Passage, respectively. Currents are measured in the entire water column and temperature and salinity are measured at three depths at these two stations. We plan to incorporate their measurements into the 2002-2003 model runs. However, measurements at these two stations would not provide enough information to construct the cross-shelf gradients of surface elevation, temperature and salinity. One possible remedy is to construct the boundary condition of surface elevation by assimilating the data measured by NOAA tidal gauges along the coast. This would require relatively more human effort in developing the assimilation scheme and possibly an adjoint model.

Process studies. Improving model results not only depend on making more observations for constructing better boundary conditions, but also depend on our understanding of related physical processes, for example, in response to a wind event, the spin-up time of Ekman pumping, location of the front and coastal currents during the summer. Both numerical experiments and field work could help improve and verify the model. The frontal locations and coastal currents are critical to the transport of nutrients and biota. A southward current of 30 cm s^{-1} can transport water parcels from the outfall site to Cape Cod Bay in less than 2 days, while cross-shelf water exchange is restricted by the fronts.

Lagrangian studies. The fate (trajectory) of a water parcel depends on its initial location, time released, and temporally and spatially dependent current field. Together with bio-chemical processes, the transport of water parcel determines the transport and burial locations of nutrients, metals and biota. Both numerical and field Lagrangian studies can effectively address these issues.

6. REFERENCES

Barth, J.A., 1989. Stability of a coastal upwelling front 1. Model development and a stability theorem, J. Geophys. Res. 94(C8): 10,844-856.

Bigelow, H.B. 1927. Physical oceanography of the Gulf of Maine (Part II). Bulletin of the Bureau of Fisheries, 40: 511-1027.

Blumberg, A.F. and G. L. Mellor, 1987. A description of a three-dimensional coastal ocean circulation model. In: Three-Dimensional Coastal Ocean Models, Coastal and Estuarine Sciences, Vol.4, N. Heaps (Ed.), American Geophysical Union, Washington, D.C., 1-6.

Bowden, K.F. 1983. *Physical oceanography of coastal waters.* Halsted Press, Chichester, New York. 302pp.

Butman, B., 1976. Hydrography and low frequency currents associated with the spring runoff in Massachusetts Bay Memoires. Societe Royale des Sciences de Liege, 6: 247-275.

Butman, B., M.H. Bothner, F.L. Lightsom, B.T. Gutierrez, P.S. Alexander, M.A. Martini, and W.S. Strahle, 2002, Long-term Oceanographic Observations in Western Massachusetts Bay offshore of Boston, Massachusetts: Data Repor for 1989-2000, U.S. Geological Survey Digital Data Series 74.

Casulli, V., 1990, Semi-implicit finite difference methods fro the two-dimensional shallow water equations, J. Comput. Phys., 86: 56-74.

Galperin, B., L.H. Kantha, S. Hassid and A. Rosati, 1988. A quasi-equilibrium turbulent energy model for geophysical flows. J. Atmos. Sci., 45: 55-62.

Geyer, W. R., G.B. Gardner, W.S. Brown, J. Irish, B. Butman, T. Loder, and R.P. Signell, 1992. Physical oceanographic investigation of Massachusetts and Cape Cod Bays. Massachusetts Bay Program. MBP-92-03, 497pp.

HydroQual, Inc. 2000. Bays Eutrophication Model (BEM): modeling analysis for the period 1992-1994. Boston, Massachusetts Water Resources Authority. ENQUAD 2000-02, 158pp.

HydroQual, Inc. 2003. Bays Eutrophication Model (BEM): modeling analysis for the period 1998-1999. Boston, Massachusetts Water Resources Authority. ENQUAD 2003-03, 318pp.

HydroQual, Inc. and R.P. Signell, 2001. Calibration of the Massachusetts and Cape Cod Bays Hydrodynamic Model: 1998-1999. Boston, Massachusetts Water Resources Authority.

ENQUAD 2001-12, 170pp.

Jiang, M. S. and M. Zhou, 2003. Massachusetts Bay Hydrodynamic Model and Water Quality Model results in 1998-99: Comparison Report between HydroQual and University of Massachusetts Boston Runs. Boston, Massachusetts Water Resources Authority. ENQUAD 2003-10, 42pp.

Jiang, M. S. and M. Zhou, 2004a. The summer Ekman pumping and its implications to the deep water renewal in Massachusetts and Cape Cod Bays. Proceedings of the 8th Estuarine Coatal Modelling. San Francisco. 11-3-2003.

Jiang, M.S. and M. Zhou, 2004b. Calibration of the Massachusetts and Cape Cod Bays water quality model: 2000-2001. MWRA ENQUAD 2004-09. 90pp.

Large, W.G. and S. Pond, 1981. Open ocean momentum flux measurements in moderate to strong winds, J. Phys. Oceanogr. 11: 324-336.

Lermusiaux, P. F. J., 2001. Evolving the subspace of the three-dimensional multiscale ocean variability: Massachusetts Bay, J. Mar. Sys., 29: 385-422.

Libby P.S., L.A. McLeod, C.J. Mongin, A.A. Keller, C.A. Oviatt, and J.T. Turner, 2002. Semiannual water column monitoring report: February – June 2001. Boston: Massachusetts Water Resources Authority. Report ENQUAD 2002-10. 559pp.

Lynch, D. and C. Naime, 1993.The M2 tide and its residual on the outer banks of the Gulf of Maine, J. Phys. Oceanogr., 23: 2222-2253.

Lynch, D.R., Naimie, C.E. and Werner, F.E., 1996. Comprehensive coastal circulation model with application to the Gulf of Maine. Cont. Shelf Res., 12: 37-64.

Mellor, G. and T. Yamada, 1982. Development of a turbulence closure model for geophysical fluid problems, Rev. Geophys. Space Phys., 20: 851-875.

Shapiro, R., 1975. Linear filtering, Mathematics of Computation, 29, 1094-1097

Signell, R.P., H.L. Jenter, and A.F. Blumberg, 1996. Circulation and effluent dilution modeling in Massachusetts Bay: model implementation, verification and results. USGS Open File Report 96-015, U.S. Geological Survey, Woods Hole.

Smagorinsky, J. 1963. General circulation experiments with the primitive equations: I. The basic experiment. Monthly Weather Review, 91: 99-164.

Smolarkiewicz, P. K., 1984: A fully multidimensional positive definite advection transport algorithm with implicit diffusion. *J. Comput. Phys.*, 54: 325-362.

Weller, R., D. Rudnick and N.J. Brink, 1995. Meteorological variability and air-sea fluxes at a closely spaced array of surface moorings. J. Geophys. Res., 100: 4867-4883.

Werme, C. and C.D. Hunt, C. D. 2002, 2001 outfall monitoring overview..Boston: Massachusetts Water Resources Authority. ENQUAD 2002-18, 84pp.

Xue, H. J., F. Chai, and N. R. Pettigrew, 2000. A model study of the seasonal circulation in the Gulf of Maine. J. Phys. Oceanogr., 30: 1111-1135.

Yu, X.-R., T. Dickey, J. Bellingham, D. Manov, and K. Streitlien, 2002. The application of autonomous underwater vehicles for interdisciplinary measurements in Massachusetts and Cape Cod Bays. *Cont. Shelf Res.*, 22: 2225–2245.

Zhou, M. 2002. Test results of the Massachusetts Bay hydrodynamic model (Year 1994), University of Massachusetts Boston, Department of Environmental, Coastal and Ocean Sciences, ECOS 2002-2, 35 pp.

Massachusetts Water Resources Authority
Charlestown Navy Yard
100 First Avenue
Boston, MA 02129
(617) 242-6000
http://www.mwra.state.ma.us